Copy 6
RM L55I21

NACA

RESEARCH MEMORANDUM

FLIGHT MEASUREMENTS OF SECTION EFFICIENCY, THRUST, AND POWER OF A SUPERSONIC-TYPE PROPELLER AT MACH NUMBERS TO 0.9

By Jerome B. Hammack and Thomas C. O'Bryan

Langley Aeronautical Laboratory
Langley Field, Va.

NATIONAL ADVISORY COMMITTEE
FOR AERONAUTICS

WASHINGTON

January 11, 1956

[redacted]

NATIONAL ADVISORY COMMITTEE FOR AERONAUTICS

RESEARCH MEMORANDUM

FLIGHT MEASUREMENTS OF SECTION EFFICIENCY, THRUST, AND POWER OF A SUPERSONIC-TYPE PROPELLER AT MACH NUMBERS TO 0.9

By Jerome B. Hammack and Thomas C. O'Bryan

SUMMARY

Flight tests have been made on a supersonic-type propeller designed for a forward Mach number of 0.95, advance ratio of 2.2, and power coefficient of 0.26. Power and thrust distributions and section efficiency were determined over a range of forward Mach numbers to 0.9 in level flight.

At an advance ratio of 2.2, forward Mach number of 0.9, and power coefficient of 0.21, blade-section efficiencies were measured to be a maximum of 83 percent. Measured thrust distributions are of uniform shape with no thrust breakdown apparent. These features are generally associated with efficient operation. Power distributions which show section power absorption are also presented.

INTRODUCTION

A flight test program to study the operation of a series of propellers under representative conditions extending from zero to near-sonic forward Mach numbers has been initiated as a joint Air Force-Navy-NACA effort. The purposes of the program are to study problems which are not adaptable to wind-tunnel research, to evaluate the effects on the aerodynamic characteristics of design compromises necessary to obtain serviceable flight installations, to verify results of tunnel and theoretical investigations, and to explore and define (through actual flight experience) problems which may be studied in detail by subsequent ground research.

The tests reported herein are concerned with the problem of the effect of design advance ratio on the characteristics of propellers

intended to operate at high-subsonic (0.95) flight Mach numbers. The blades are designed for an advance ratio of 2.2 and are of the supersonic type, characterized by the fact that all sections operate at supersonic resultant Mach numbers in order to attain an optimum advance angle for maximum profile efficiency. The philosophy behind the supersonic-propeller-design concept has been described in several reports, for example, references 1 to 3. Very little flight experience is presently available on this type of propeller and considerable interest centers around the question of whether flight efficiencies comparable with predicted efficiencies are available. These propeller blades are considered to represent the best current practice in achieving a compromise between aerodynamic and structural considerations in order to obtain adequate service capabilities.

The propeller research vehicle used for the program is a McDonnell XF-88B airplane modified by installation of a turboprop engine in the nose. The propeller research vehicle is instrumented to provide both force-test data and slipstream-survey data. The survey data provide information relative to section operation, that is, the radial distribution of power absorption, thrust, and section efficiency. This is the first time that section efficiencies have been measured on a supersonic-type propeller. Because of the generally accepted uncertainty of the performance of propellers in transonic flight, this paper is being presented to show section efficiencies measured in flight under these conditions. Difficulties with the force-measuring system preclude inclusion of total-efficiency data in the present paper.

SYMBOLS

A	area of propeller disk, sq ft
b	blade chord, ft
c_p	specific heat at constant pressure, 6006 ft-lb/slug/$^\circ$F
c_P	propeller power coefficient, $\frac{P}{\rho n^3 D^5}$
D	propeller diameter, ft
g	acceleration due to gravity, 32.2 ft/sec^2
H	total pressure, lb/sq ft
ΔH	total-pressure rise in slipstream, lb/sq ft

[redacted]

h	blade thickness, ft
J	propeller advance ratio, V/nD
M	free-stream Mach number
M_t	propeller-tip Mach number
M_x	blade section Mach number at design forward Mach number of 0.95
n	propeller rotational speed, rps
P	power, ft-lb/sec
dP	incremental power, ft-lb/sec
dHP	incremental horsepower, dP/550
p	static pressure, lb/sq ft
R_g	perfect gas constant, 53.3
r	radius of an element on blade
r_s	radial dimension to survey measurement
R	propeller radius, ft
T	thrust, lb
dT	incremental thrust, lb
V	velocity, ft/sec
ΔV	incremental velocity change of propeller slipstream, ft/sec

$x = r/R$

$x_s = r_s/R$

t	free-stream static temperature outside propeller slipstream, $^{\circ}F$ absolute
$\Delta\theta$	stagnation temperature rise in propeller slipstream, $^{\circ}F$
β	blade angle, deg
γ	ratio of specific heats, 1.4

[redacted]

η' propeller section efficiency

ρ density of air, slugs/ft^3

Subscripts:

l local conditions

∞ free-stream conditions

s pertains to survey rake

TEST EQUIPMENT

Research Vehicle

The propeller flight test vehicle is a McDonnell XF-88B airplane modified by installation of a turboprop engine in the nose (fig. 1). The test vehicle is capable of Mach numbers in excess of 0.9 in level flight and capable of reaching supersonic Mach numbers in shallow dives. The performance of the test vehicle is essentially independent of the characteristics of the test propeller configuration. General specifications of the test vehicle are as follows:

Length, ft	58
Gross weight, lb	22,200
Wing span, ft	39.7
Wing area, sq ft	350.0
Wing aspect ratio	4.49
Wing sweepback angle, deg	35
Primary power plants (two)	J-34-WE 34 jet engines with afterburners
Propeller power plant	XT-38-A-5
Propeller rotational speeds available, rpm	1,700, 3,600, 6,000
Maximum allowable propeller diameter, ft	10

The three propeller rotational speeds available are obtained by interchangeable gear boxes. In the tests reported on herein, the gear box for 3600 rpm was used.

Instrumentation

Slipstream survey measurements.- A slipstream-survey rake was mounted on each side of the airplane nose; the pressure probes were located 0.6 propeller diameter downstream of the propeller plane; and

[redacted]

the temperature probes were located 0.7 propeller diameter downstream. Each survey rake consisted of a streamlined strut, on which were mounted 23 total- and static-pressure probes and 10 resistance-type total temperature thermometers. The probes are alined on and parallel to the propeller thrust axis. The locations of the pressure probes and thermometers are presented in table I. A photograph of the installation is shown in figure 2, and a sketch of a typical probe is shown in figure 3.

The total pressure and static pressure in the propeller slipstream was measured by the individual survey probes, referenced to a probe located sufficiently outboard as to be out of the influence of the slipstream. Tare values of pressure were measured in flight with a dummy 60° spherical spinner with the propeller removed. All pressure measurements used in this paper for determination of efficiency were obtained sufficiently outboard so that no tare corrections were necessary. The slipstream-survey pressure system has an appreciable time lag; however, it was possible to obtain the data of this paper in level flight so that lag corrections were unnecessary.

The stagnation-temperature rise in the propeller slipstream was measured utilizing resistance bulb thermometers. The thermometers were miniature versions of the bulb of reference 4 and otherwise differed only in mounting of the resistance winding. The resistance winding was wrapped around a copper cylinder having 0.001-inch wall thickness.

The resistance bulbs were mounted on thin streamlined struts attached to the bottom of the right and left survey rakes, at 10 radial locations, in the propeller slipstream (fig. 3 and table I). Two reference bulbs, one for each set of rake bulbs, was located underneath the right wing of the airplane (outside the propeller slipstream). The temperature measuring system incorporated a wheatstone bridge in which the reference resistance bulb was balanced alternately with each of the resistance bulbs on the survey rake. The difference in resistance between the reference and rake bulbs was calibrated directly in degrees Farenheit for values of total stream temperature expected in flight and was recorded on an oscillograph. In order to complete the system, another temperature bulb was located alongside the reference bulbs to measure free-stream total temperature.

Flight calibration of temperature system.- The recovery factor and time lag at sea level of the temperature bulbs was determined from laboratory calibration to be approximately 99.5 $\pm$ 0.5 percent and 0.5 second at a Mach number of 0.77. A flight calibration of the system without a propeller installed was performed to determine difference in recovery factor between the individual thermometers and the reference thermometer. This calibration resulted in a temperature distribution which deviated from zero as a result of the difference in recovery

[redacted]

factor and difference in local Mach number at the various rake bulbs and the reference bulb.

A typical radial distribution of temperature rise in degrees Farenheit as a function of $(r_s/R)^2$ is shown in figure 4 for Mach numbers of 0.66 and 0.94. The temperature distortion indicated by the inboard measurements (from $(r_s/R)^2 = 0.7$ inboard) is due to the wake of the large 60° spherical spinner. This distortion results from the radial conduction of heat and is a usual phenomenon in a boundary layer where the wall temperature is higher than the static temperature. The extent of this distortion is, however, very large. Measurements of temperature rise in the inboard region have not been used in this paper for efficiency determination because of the difficulty in experimental determination of the effective recovery factor. The deviation of the temperature measurements from zero has been considered as being due to difference in recovery factor. The flight calibration was obtained for Mach numbers up to approximately 0.80. The indicated recovery factors were constant up to this Mach number and were assumed constant for all higher Mach numbers used in this paper. A further limitation on the use of the temperature measurements, at the present time, restricts its use to conditions where there is no appreciable change in temperature with time.

General airplane instrumentation.- The source of static and total pressure for the airspeed system was a high-speed pressure tube mounted one tip chord ahead of the right wing tip of the airplane. The impact pressure and static pressure were recorded with a standard NACA airspeed recorder. This airspeed system is accurate to 0.005 in Mach number for Mach numbers up to 0.97.

Test Configuration

The test configuration consisted of three blades and a 60° spherical spinner (figs. 1, 2, and 5). Blade-form curves are shown in figure 6. The propeller is 7.2 feet in diameter and is essentially a 0.6-scale model of a 12-foot-diameter propeller designed to operate at an advance ratio of 2.2, forward Mach number of 0.95, and an altitude of 40,000 feet. The power coefficient during the tests was approximately 0.21, which corresponds to about 80 percent of the design power coefficient of 0.26. These blades incorporate NACA 16-series symmetrical airfoil sections. The solidity of the propeller is 0.154 at the 0.7 radial station.

The propeller was tested in conjunction with a spherical spinner. This type of spinner, in which the contour at the blade-spinner juncture is spherical, is used in the research program to obtain a mechanically simple blade-spinner seal and to maintain an essentially

constant juncture geometry under all conditions of operation. The spherical spinner produces high induced velocities in the plane of the propeller (ref. 5), whereas the blades were designed to operate with a spinner producing relatively low induced velocities. In this respect, therefore, the test configuration may not represent an optimum design.

Test Procedure

The tests reported on herein were obtained in level flight at 20,000 feet. The turboprop was air-started at 5000 feet to aid in the climb to 20,000 feet. The propeller was adjusted to govern at 3500 rpm (corresponding to 97-percent rated turbine speed) and turbine inlet temperature set at 790° C to 800° C. This value of turbine inlet temperature corresponded to near maximum operating conditions. The airplane was accelerated to the maximum test Mach number of 0.9 by means of increased main jet power and afterburner operation.

DATA REDUCTION

Section Power

Section power was determined from the stagnation temperature rise and pressures in the slipstream by using the general energy equation:

$$P = c_p(\rho A V_l)\Delta\theta \tag{1}$$

If an annulus element dA is considered and the mass flow arranged in terms of quantities measured by the slipstream survey, the equation is as follows:

$$dP = c_p\sqrt{\frac{\gamma}{gR_g}}\frac{p_l M_l}{\sqrt{t_l}}\Delta\theta\ dA \tag{2}$$

or

$$\frac{dP}{dx_s^2} = c_p\sqrt{\frac{\gamma}{gR_g}}\frac{p_l M_l}{\sqrt{t_l}}\Delta\theta\pi R^2 \tag{3}$$

In determination of mass flow, the free-stream static temperature was used instead of local static temperature t_l. The use of the free-stream static temperature results in a maximum error of 0.5 percent.

The rake surveys a line in a plane of the slipstream that is not exactly perpendicular to the slipstream because of the rotation. No correction for this angularity has been applied to the mass flow.

[redacted]

Incremental power is considered to be accurate to ±3 percent as a result of the assumptions involved in mass-flow determination and temperature recovery factor.

Elemental thrust.- Elemental thrust was determined from measurements of total-pressure rise in the slipstream in conjunction with free-stream conditions. From reference 6 the equation for incremental thrust is

$$dT = 7p_l\left[\left(\frac{H_l}{p_l}\right)^{2/7} - 1\right]\left[\frac{\left(H_l^{2/7} - p_\infty^{2/7}\right)^{1/2} - \left(H_\infty^{2/7} - p_\infty^{2/7}\right)^{1/2}}{\left(H_l^{2/7} - p_l^{2/7}\right)^{1/2}}\right]dA \quad (4)$$

Under conditions of survey covered by this paper this equation can be reduced to the short-form equation, also found in reference 6,

$$dT = \left(\frac{p_\infty}{H_\infty}\right)^{5/7}\Delta H\, dA \quad (5)$$

or

$$\frac{dT}{dx_s^2} = \pi R^2\left(\frac{p_\infty}{H_\infty}\right)^{5/7}\Delta H \quad (6)$$

Section values of thrust were calculated by both short and long forms and were found to agree within the accuracy of the measurements. Consequently, the section thrusts of this paper have been calculated by the short-form equation. As the total-pressure probes are insensitive to small changes in angle, the thrust calculated in this fashion does not account for rotation of the slipstream. This correction, as was used in this paper, is a function of the power and can be expressed as

$$\text{Thrust correction} = -\frac{(cp)^2}{8\pi}\rho\left(\frac{\Delta\theta}{nx}\right)^2 \quad (7)$$

Section thrust determined from the slipstream survey is considered to be accurate to ±2.0 percent; this accuracy results primarily from instrumentation and data-reduction accuracy.

[redacted]

Section Efficiency

Propeller efficiency is the ratio of thrust produced to power absorbed times the true speed of the airplane. Section efficiency can be determined from equations (2) and (6) and the velocity of the airplane.

$$\eta' = \frac{dT/dx_s^2}{dP/dx_s^2} V_\infty \tag{8}$$

The section thrust and power for determination of section efficiency must be the values that represent the same radial element of the slipstream and represent the average of right and left survey measurements. The thermometers are located farther downstream than the pressure probes and the plan form of the fuselage nose has appreciable slope, as shown in figure 7. As a result of this, it is necessary to shift the temperature distribution outboard $0.05x_s^2$ to represent the same section of the slipstream. The section efficiency is considered to be accurate to approximately ±3 percent; this accuracy is based primarily on the accuracy of the thrust and power measurements.

RESULTS AND DISCUSSION

Variations in section efficiency at a selected radial station, advance ratio, and tip Mach number for forward Mach numbers up to 0.9 are shown in figure 8. The blade section efficiency at an x_s^2 of 0.8 for a forward Mach number of 0.9 is 82 percent. At this point the advance ratio is very nearly the design value of 2.2, the tip Mach number is 1.57, and the power coefficient is 0.21.

Thrust-distribution curves plotted as total-pressure rise against x_s^2 for the blade design are shown in figure 9. These distributions are of a smooth uniform shape and are similar to those produced by an efficiently operating subsonic propeller. There are no dips characteristic of thrust breakdown experienced by subsonic-type propellers operating with tip Mach number in the region of Mach number 1.0. The distributions in the inboard regions are complicated by the wake of the large 60° spherical spinner. As reported in reference 5, the flow was sufficiently disturbed by the dummy spinner so as to cause the airplane to buffet at Mach numbers above 0.71. Tare values obtained with the dummy nonrotating spinner are shown to indicate a qualitative picture of the spinner effects as measured by the survey rakes. These tare curves indicate the presence of flow disturbances too large to permit reliable thrust measurements in this region.

[redacted]

Temperature distribution curves are shown in figure 10 for the range of flight Mach numbers of the test. These curves are proportional to the power distribution. From known engine operating conditions, the power was estimated to be approximately 1800 horsepower. This power corresponds to a power coefficient of 0.21 which is approximately 80 percent of the design power coefficient of 0.26. Note that the characteristic difference in thrust distribution levels between the right and left survey due to inclination of the thrust axis is also evident in the temperature distribution curves. There is also an effect of the large 60° spherical spinner in the inboard part of the temperature distributions. The temperature distributions with propeller removed and dummy spinner on are shown in figure 4.

Because of the uncertainty in applying tare curves for both total pressure and temperature distributions, the section power and thrust values are calculated only for values of x_s^2 from 0.6 on. From these values of thrust and power the section efficiencies can be calculated. Distribution of section thrust, power, and section efficiency for values of x_s^2 from 0.6 to 1.0 are shown in figure 11 for a range of Mach numbers to 0.9. The power distributions were shifted inboard by a value of x_s^2 of 0.05 to account for the difference in the position of the fuselage side at the two survey planes. In the extreme outboard range there may still be some misalinement as in this region the slope of the total-pressure rise and temperature rise is high, and a small radial shift can cause an appreciable change in value of section efficiency.

The values of section efficiency agree well with theoretical values obtained by using calculated values of maximum lift-drag ratio. For example, at a forward Mach number of 0.9, the section Mach number at x_s^2 of 0.8 is Mach number 1.5. For this Mach number a maximum lift-drag ratio of 11 is calculated for a section having a thickness ratio of 2 percent. This value of lift-drag ratio produces a section efficiency of 83 percent. The measured value of section efficiency is 82 percent as shown in figure 8. Figure 11(g) shows, however, that an efficiency of 83 percent was attained at a value of x_s^2 of 0.85. Consequently, the experimental values of section efficiency tend to bear out theoretically calculated values and these values, in general, show high efficiency at high subsonic forward Mach numbers.

CONCLUDING REMARKS

Flight tests on a supersonic-type propeller designed for a forward Mach number of 0.95, advance ratio of 2.2, and power coefficient of 0.26 show good section efficiencies. A maximum section efficiency of 83 percent was measured at a forward Mach number of 0.9. Thrust distributions

over a range of Mach numbers to 0.9 are smooth and uniform; such distributions are indicative of efficient operation. The section efficiencies reported herein verify theoretical calculations.

Langley Aeronautical Laboratory,
National Advisory Committee for Aeronautics,
Langley Field, Va., September 20, 1955.

REFERENCES

1. Smith, C. B., and Giarratana, S. A.: The Supersonic Propeller Concluding Report. Rep. R-12004-03, United Aircraft Corp. Res. Dept., Apr. 23, 1948.

2. Borst, H. V.: Aerodynamic Study of the Theory and Performance of Supersonic Propellers. Rep. No. C-2044B, Curtiss-Wright Corp. Propeller Div. (Caldwell, N. J.), Mar. 29, 1949.

3. Hammack, Jerome B.: The Aerodynamic Design of Supersonic Propellers From Structural Considerations. NACA TN 2851, 1952.

4. Lina, Lindsey J., and Ricker, Harry H., Jr.: Measurements of Temperature Variations in the Atmosphere Near the Tropopause with Reference to Airspeed Calibration by the Temperature Method. NACA TN 2807, 1952.

5. Hammack, Jerome B., Windler, Milton L., and Scheithauer, Elwood F.: Flight Investigation of the Surface-Pressure Distribution and the Flow Field Around a Conical and Two Nonrotating Full-Scale Propeller Spinners. NACA TN 3535, 1955.

6. Vogeley, A. W.: Flight Measurements of Compressibility Effects on a Three-Blade Thin Clark Y Propeller Operating at Constant Advance-Diameter Ratio and Blade Angle. NACA WR L-505, 1943. (Formerly NACA ACR 3G12.)

[redacted]

TABLE I

RAKE STATION LOCATIONS

[Total and static pressure probes at all stations]

Station number	r_s, in.	$(r_s/R)^2$	Thermometer
1	23.30	0.291	
2	24.50	.322	x
3	27.40	.402	
4	29.20	.457	x
5	31.00	.515	
6	32.00	.549	x
7	34.10	.623	
8	35.60	.679	x
9	37.00	.734	
10	38.40	.790	x
11	39.70	.845	
12	41.00	.901	x
13	42.30	.959	
14	43.50	1.014	x
15	44.70	1.071	
16	45.80	1.124	x
17	46.90	1.179	
18	48.00	1.235	x
19	50.00	1.340	
20	51.50	1.421	x
21	53.50	1.534	
22	55.50	1.651	
23	57.50	1.772	

Location of fuselage side	r, in.	$(r_s/R)^2$
At line of pressure probes	20.9	0.235
At line of thermometers	23.9	.283

[redacted]

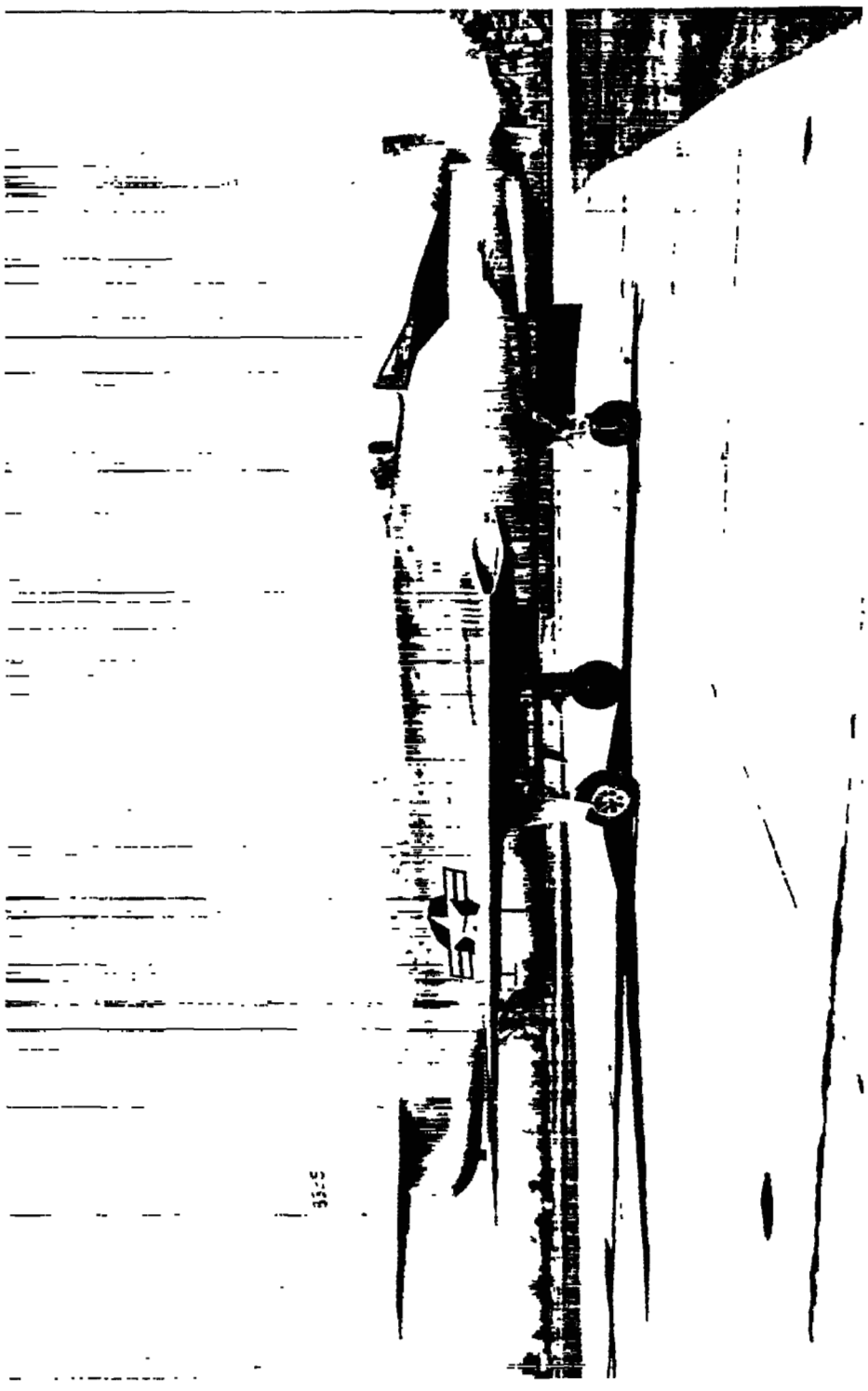

L-87394

Figure 1.- Photograph of flight test vehicle.

L-87399

Figure 2.- Photograph of slipstream survey rake installed on airplane.

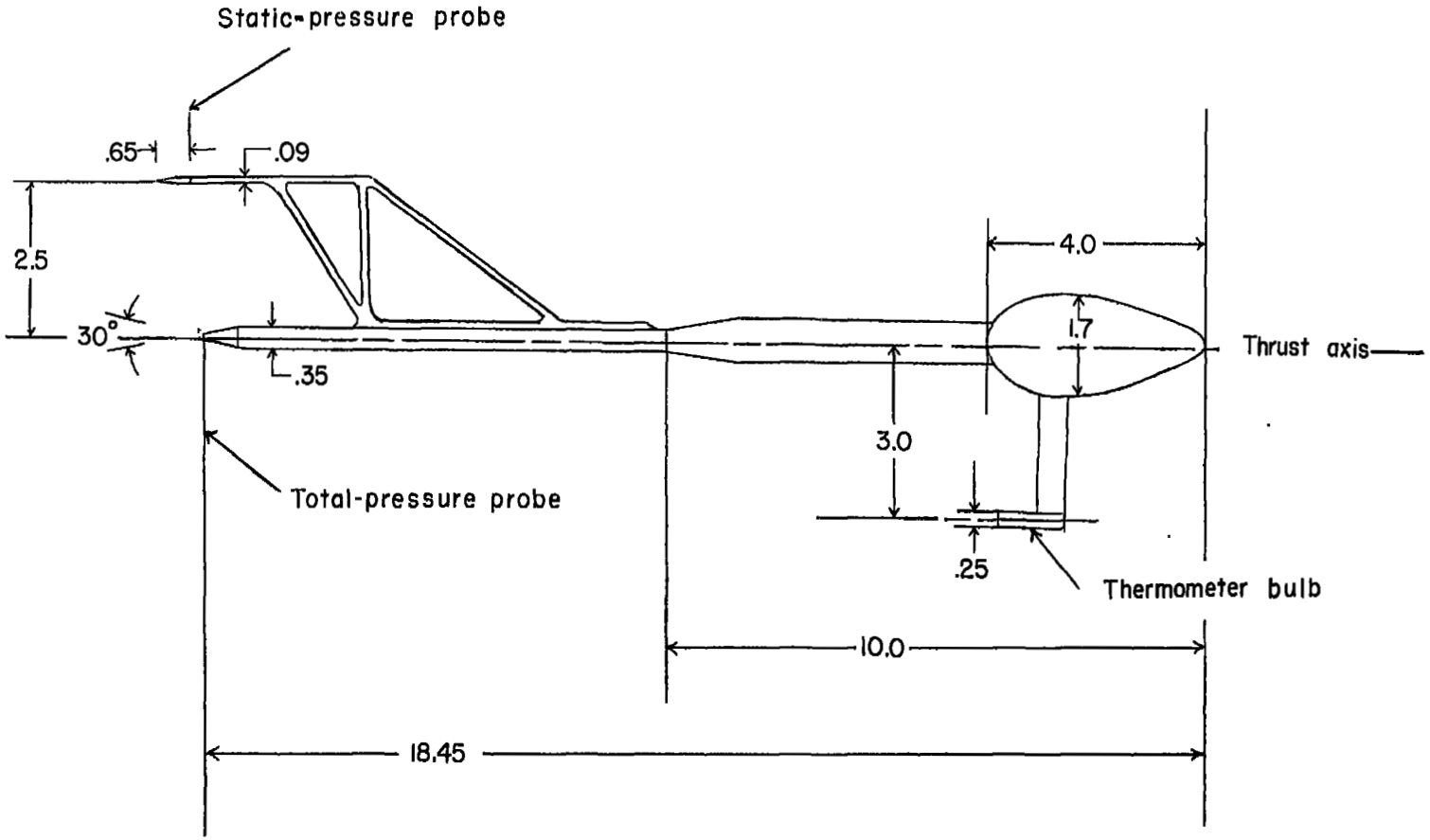

Figure 3.- Sketch of a typical slipstream survey probe. All dimensions are in inches.

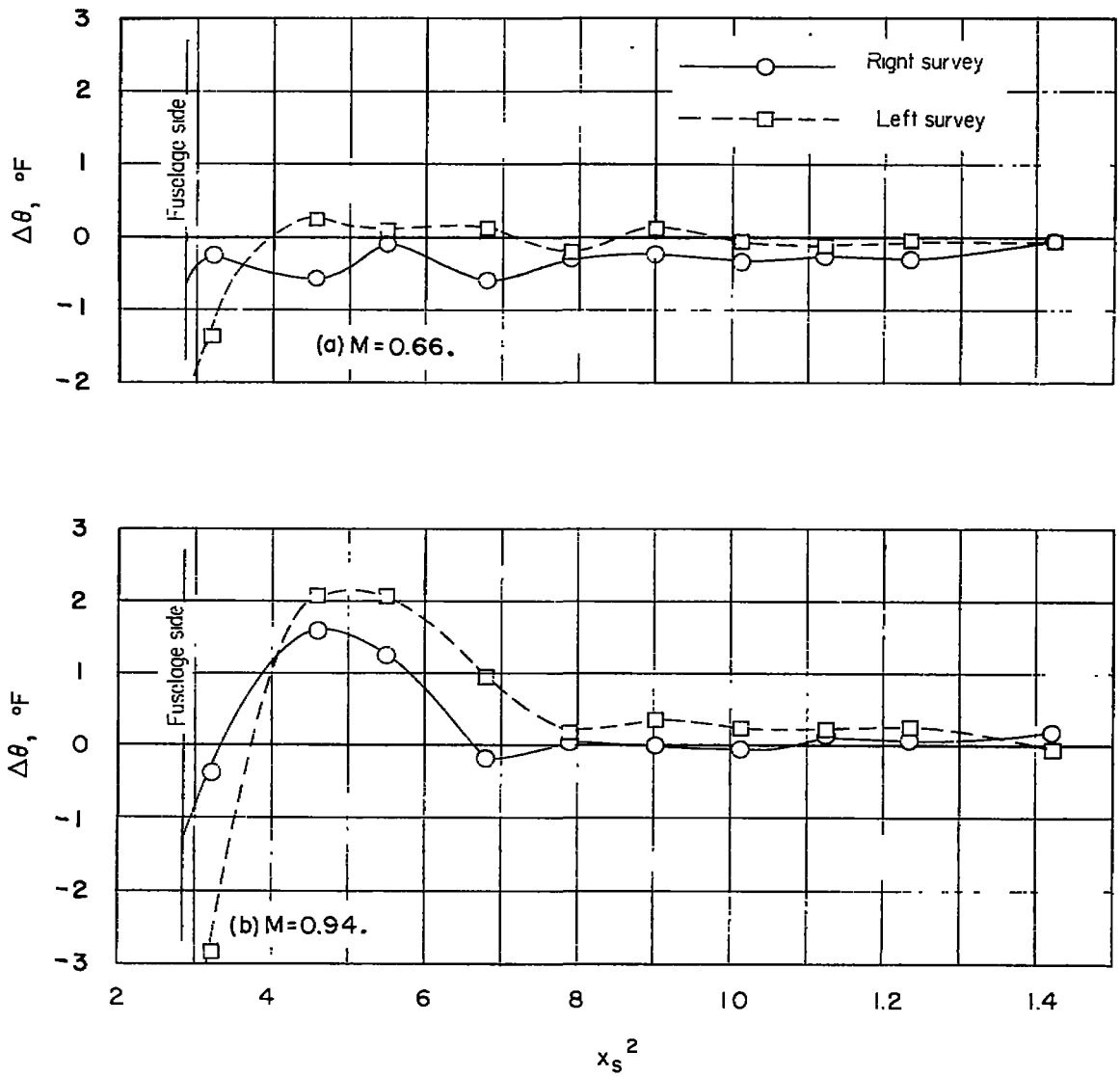

Figure 4.- Distribution of total temperature rise. No propeller installed for Mach numbers of 0.66 and 0.94.

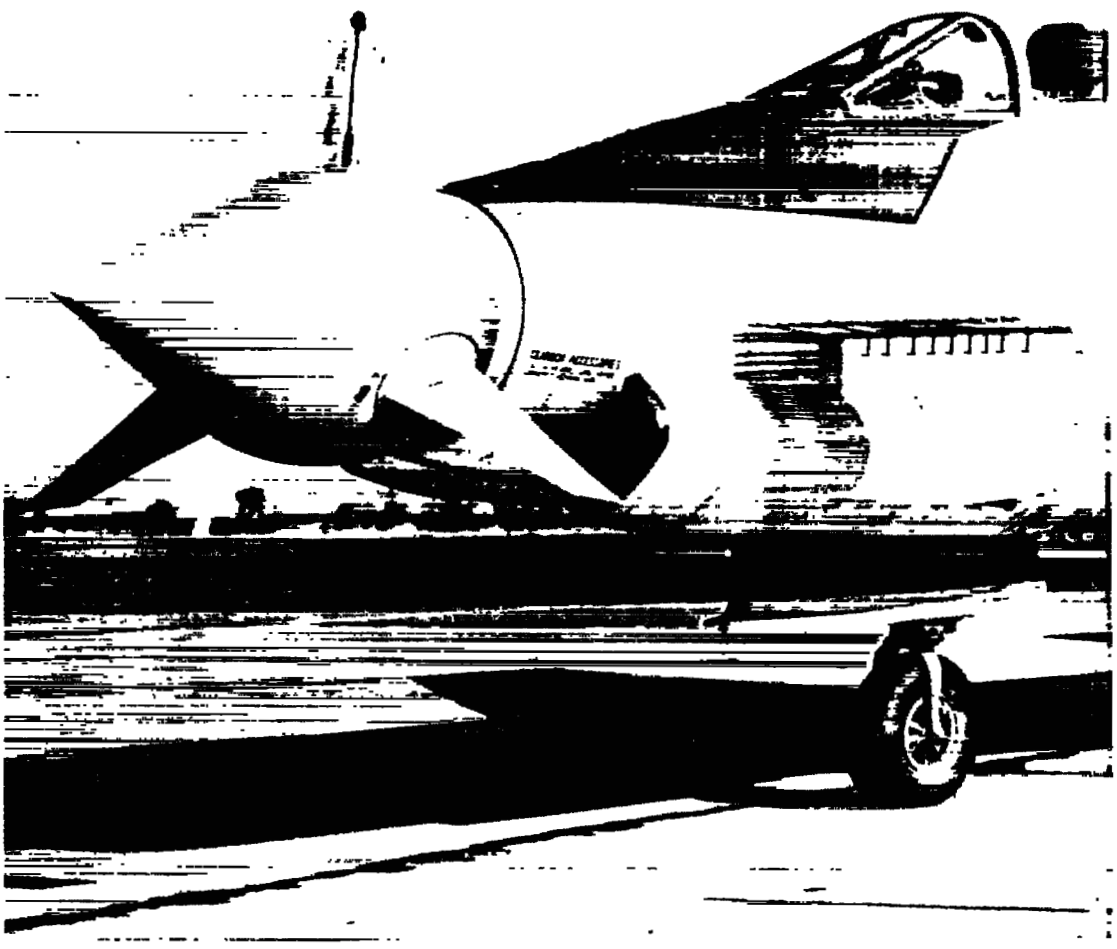

L-87397.1

Figure 5.- Photograph of test configuration showing propeller blades and 60° spherical spinner.

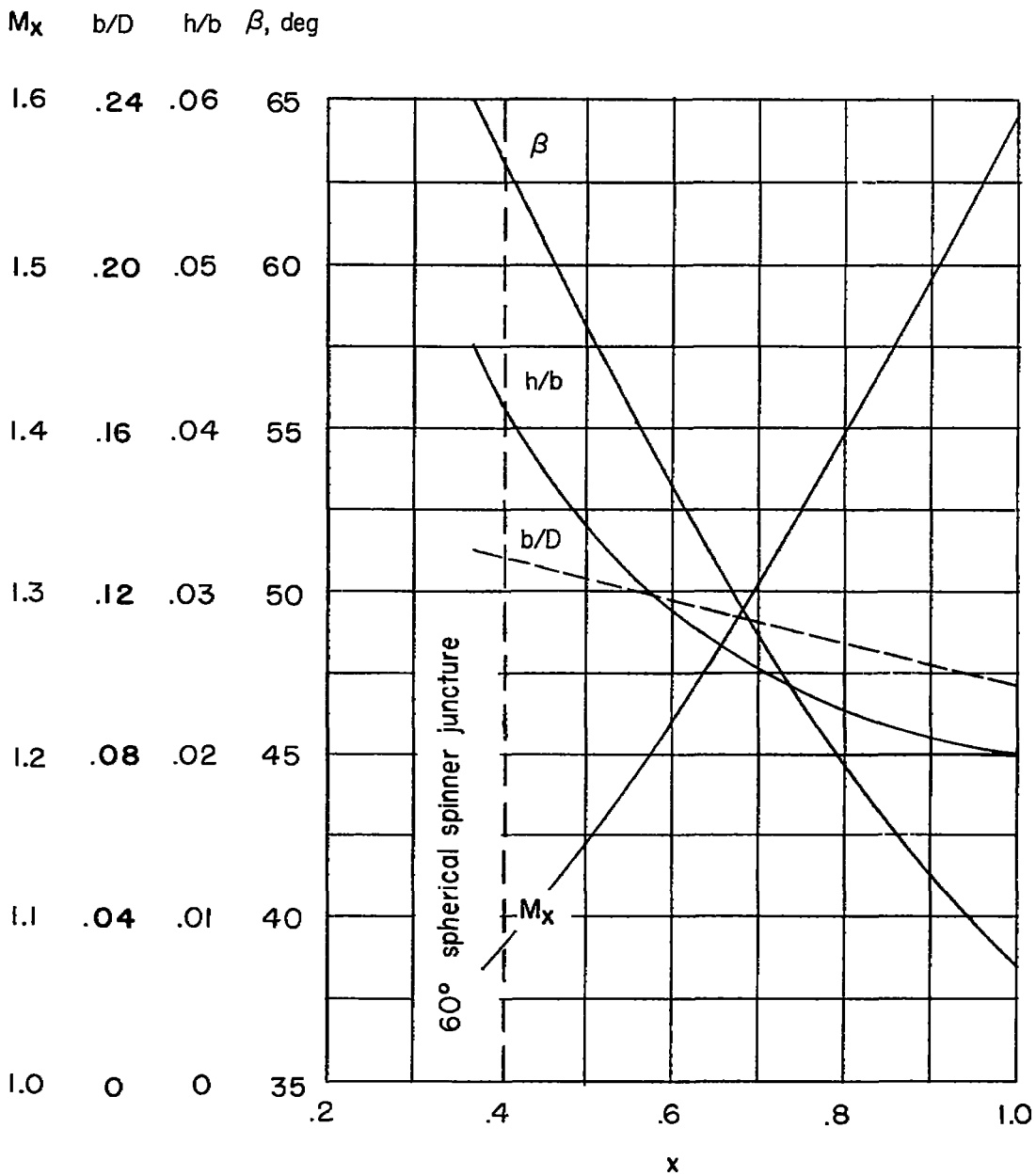

Figure 6.- Characteristics of propeller blades.

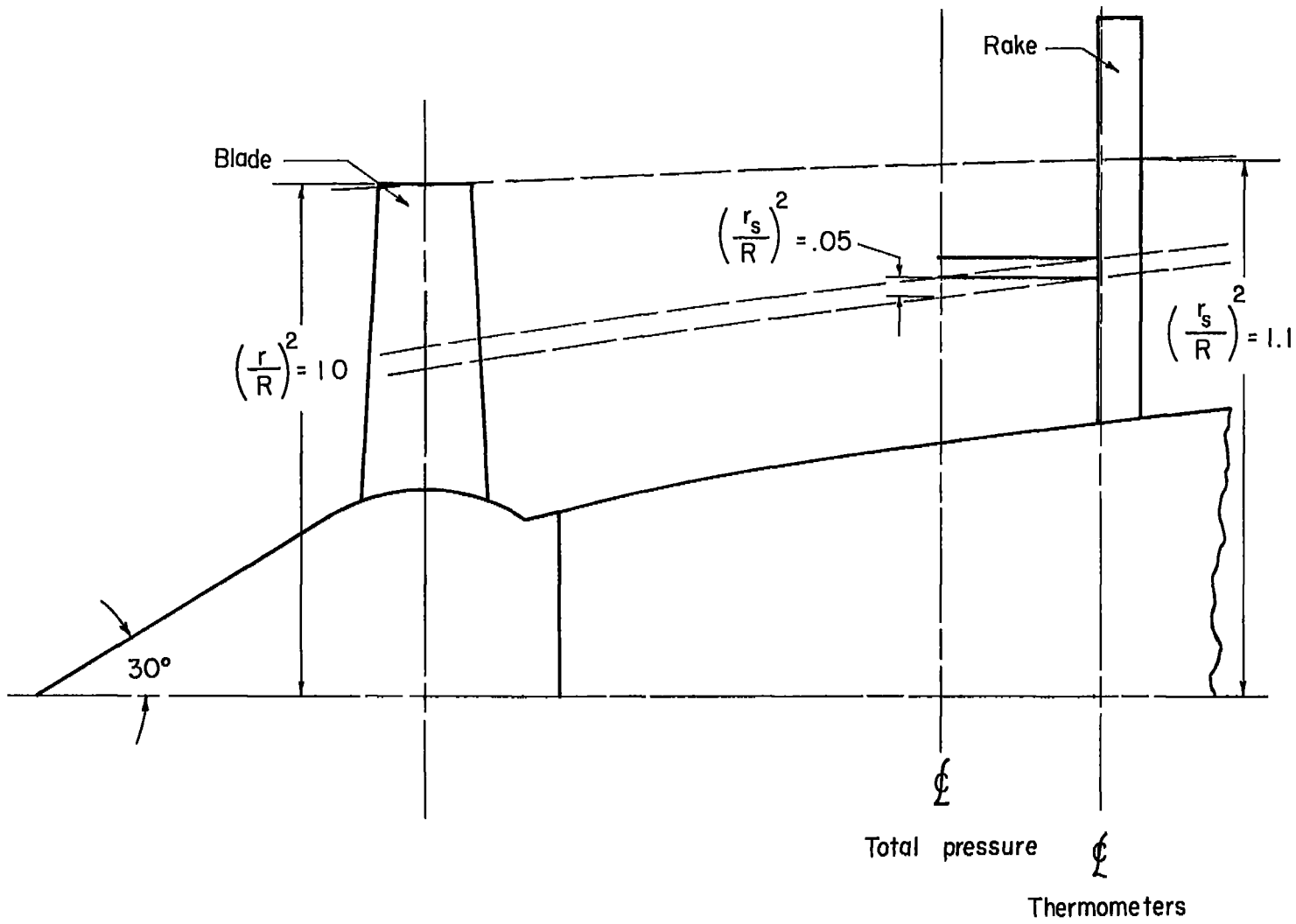

Figure 7.- Schematic diagram of rake-survey arrangement.

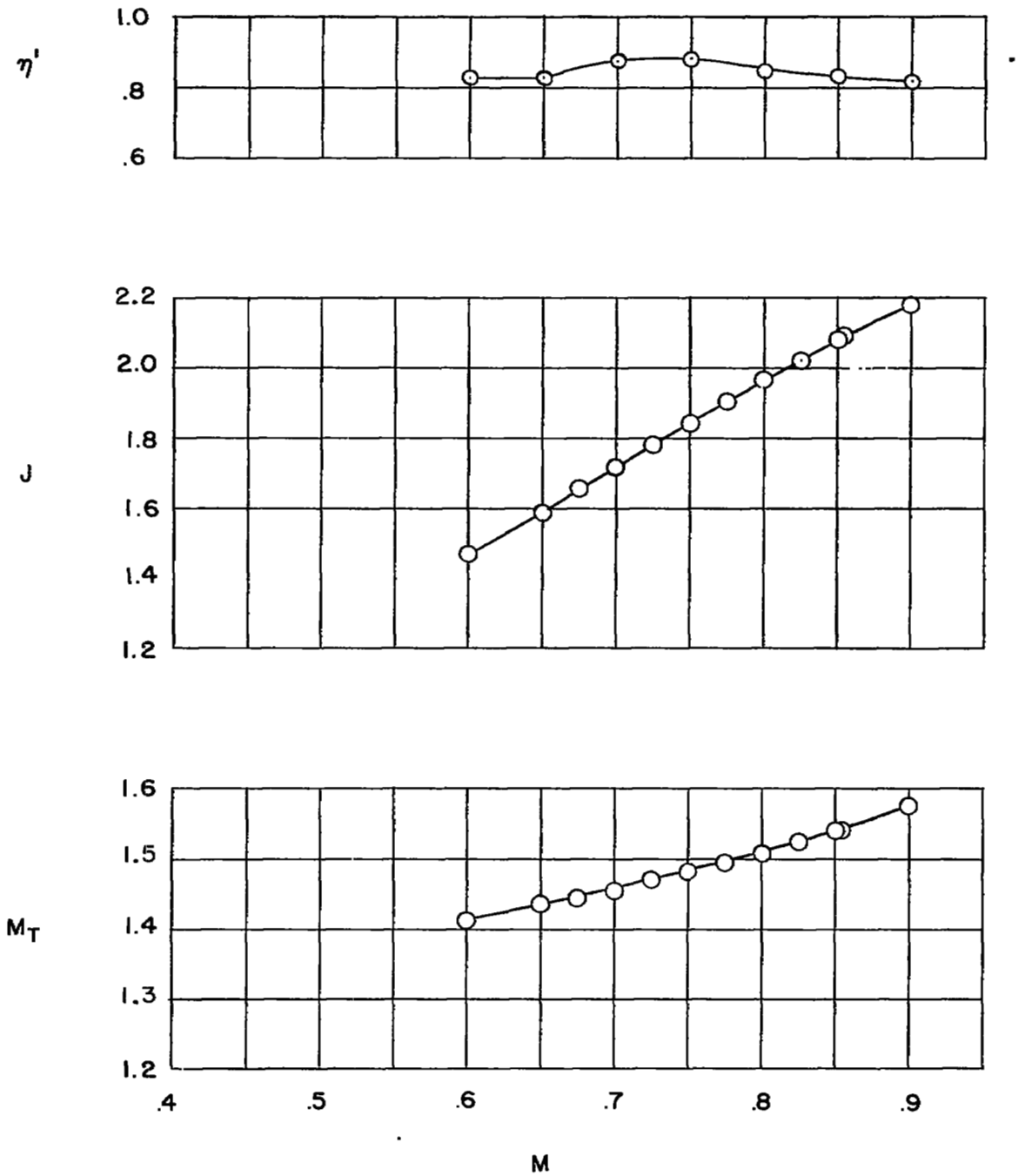

Figure 8.- Section efficiency, advance ratio, and tip Mach number for several values of forward Mach number for the test propeller. Values of η' are for $x_s^2 = 0.8$.

[redacted]

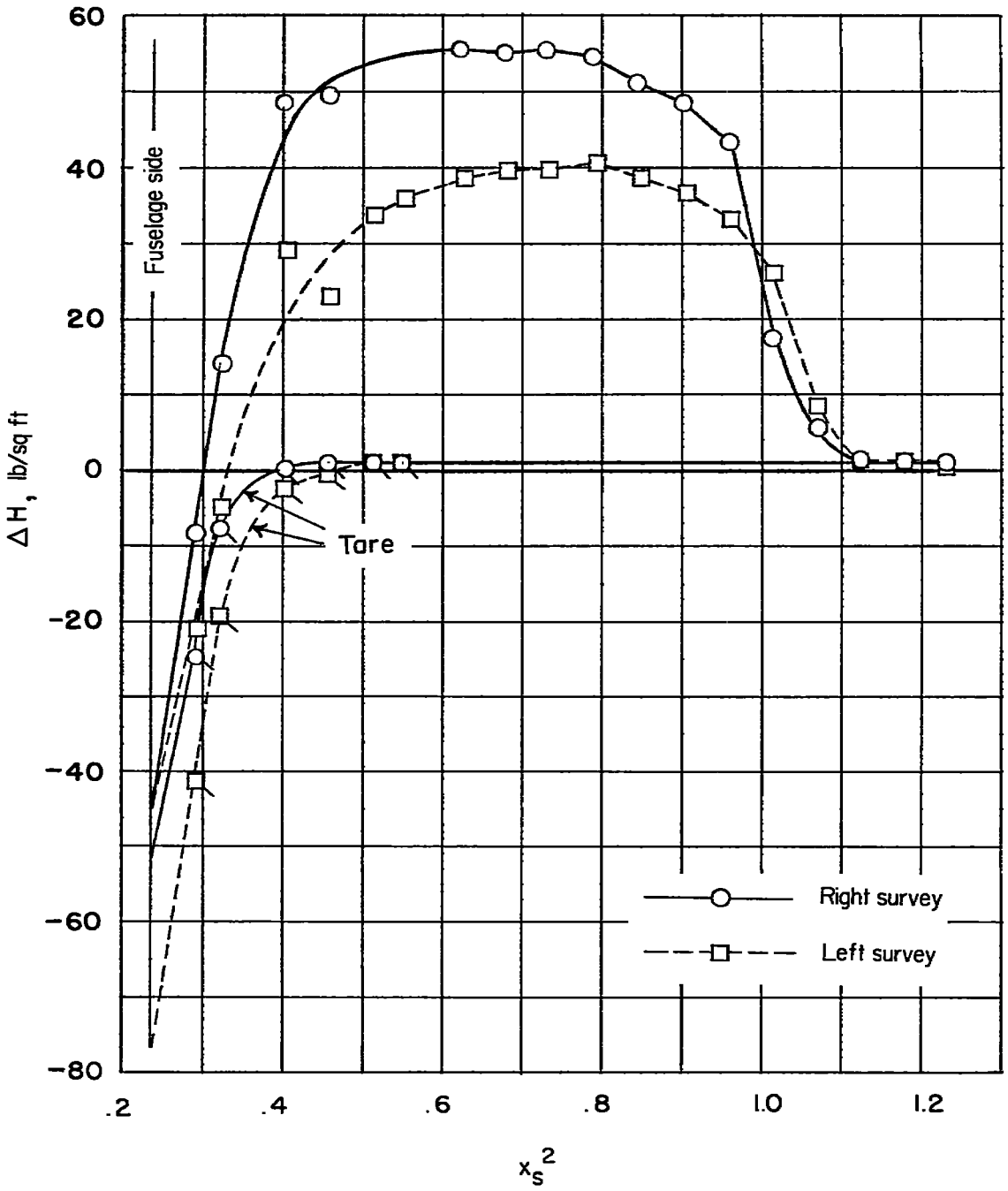

(a) M = 0.60.

Figure 9.- Distribution of total-pressure rise measured in the propeller slipstream. Propeller and 60° spherical spinner on propeller research vehicle.

[redacted]

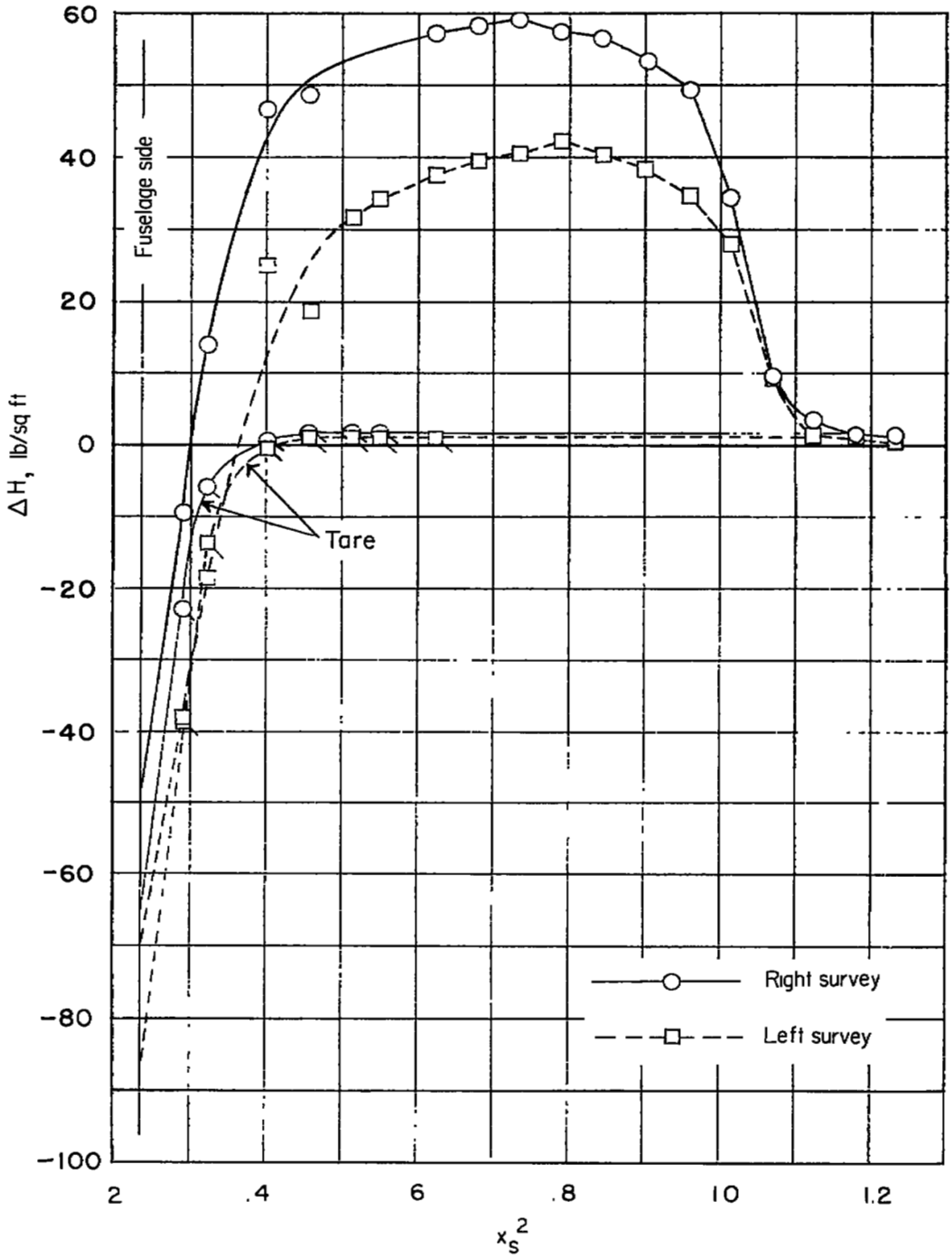

(b) M = 0.65.

Figure 9.- Continued.

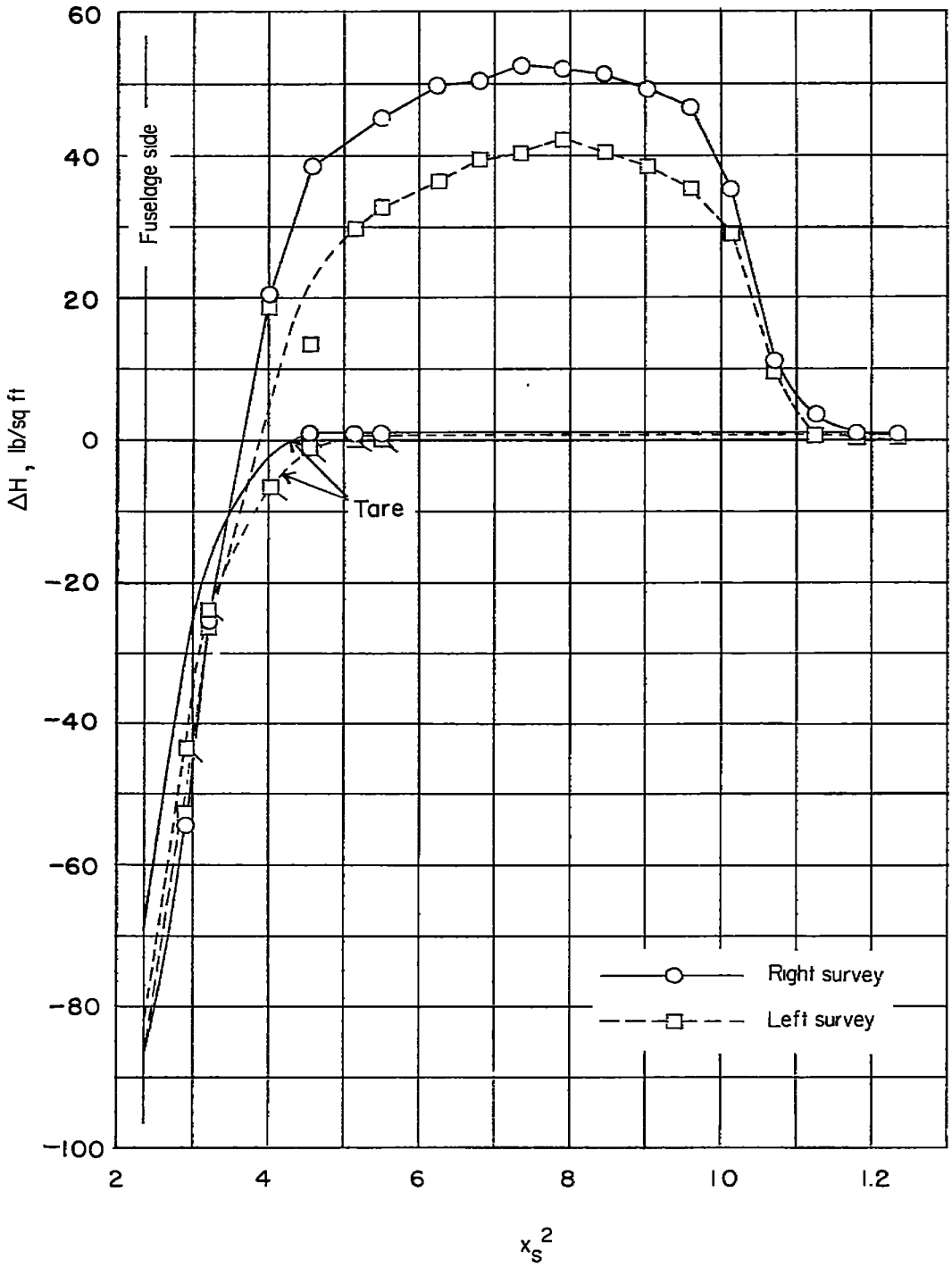

(c) M = 0.70.

Figure 9.- Continued.

[redacted]

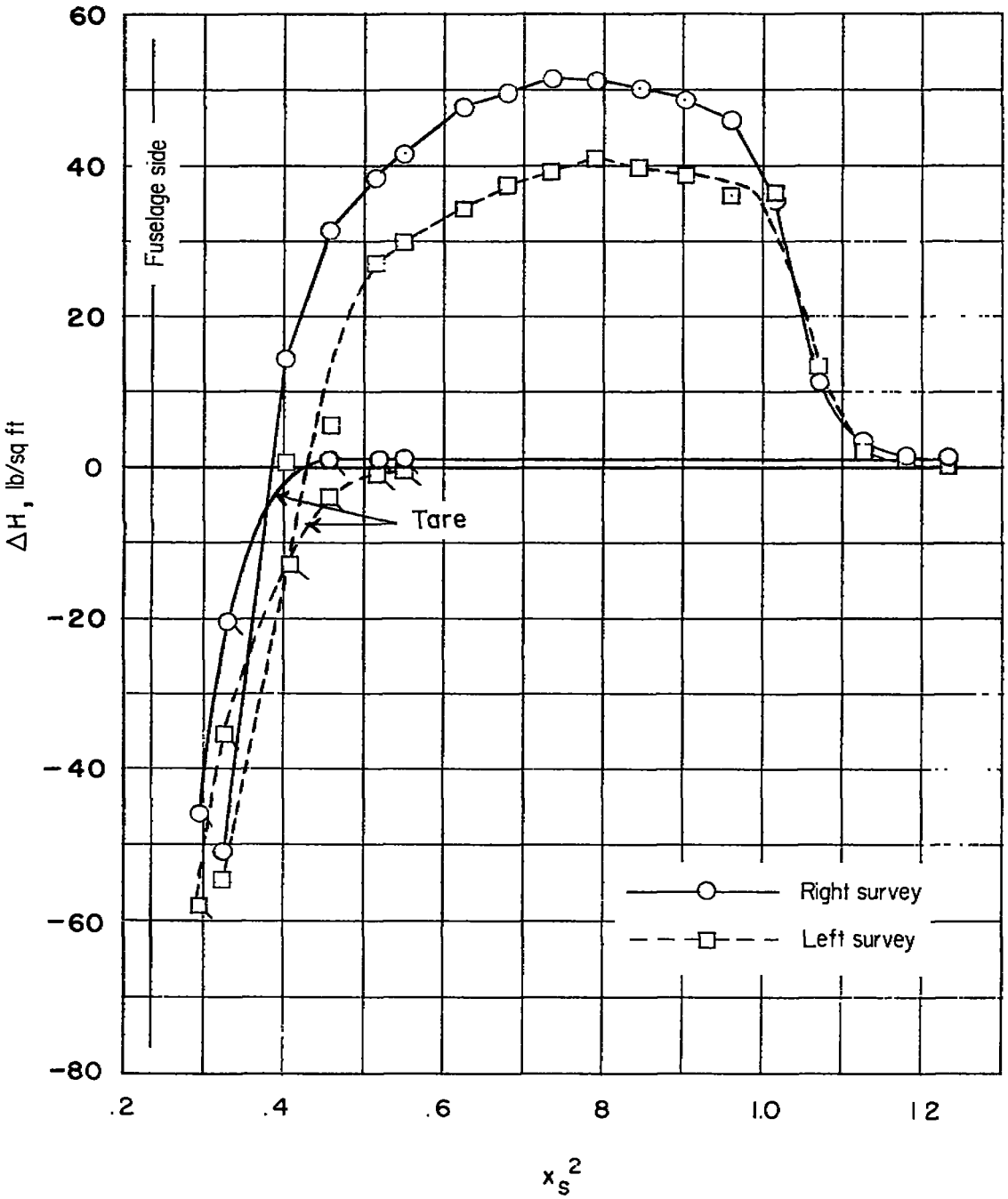

(d) M = 0.75.

Figure 9.- Continued.

[redacted]

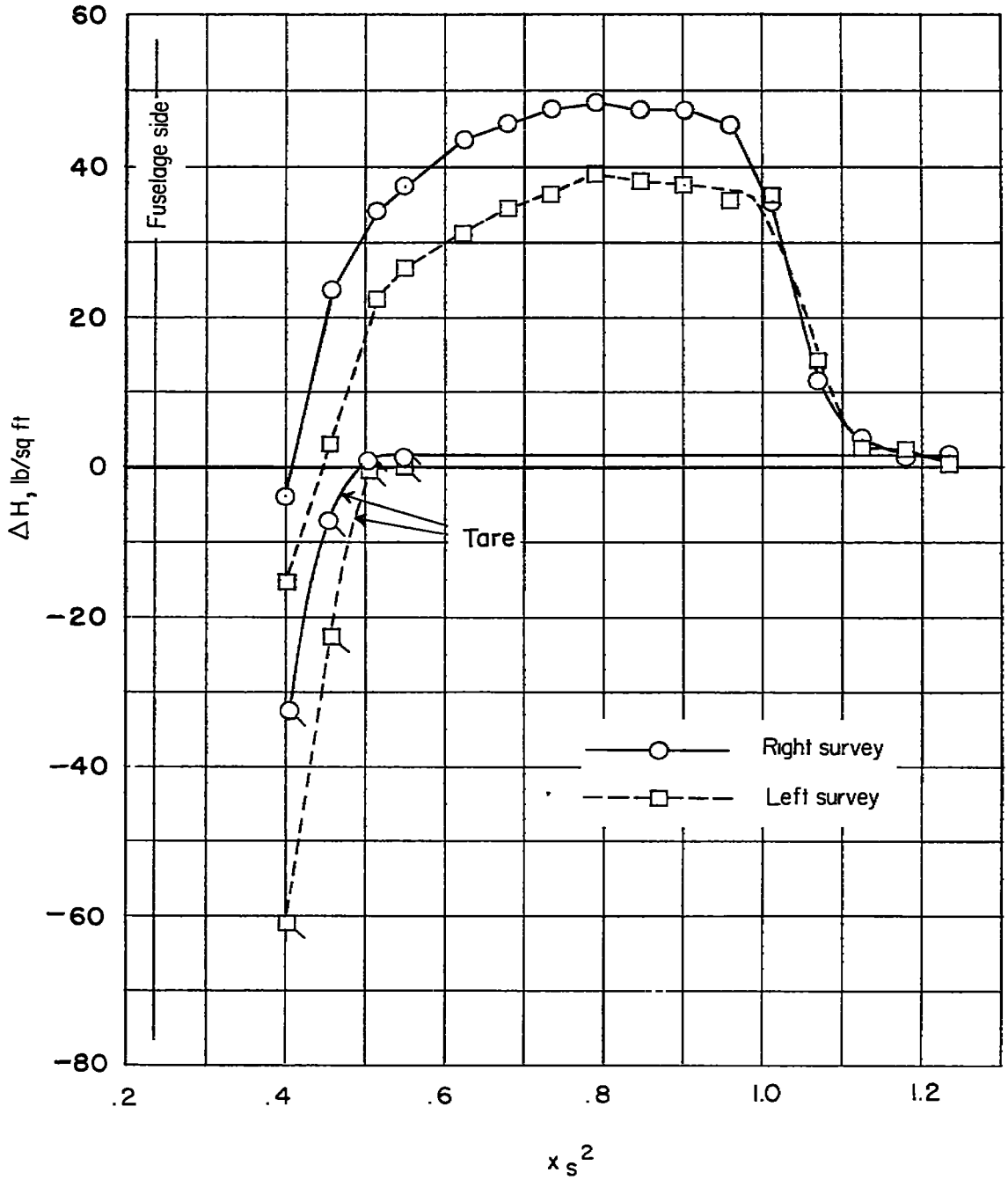

(e) M = 0.80.

Figure 9.- Continued.

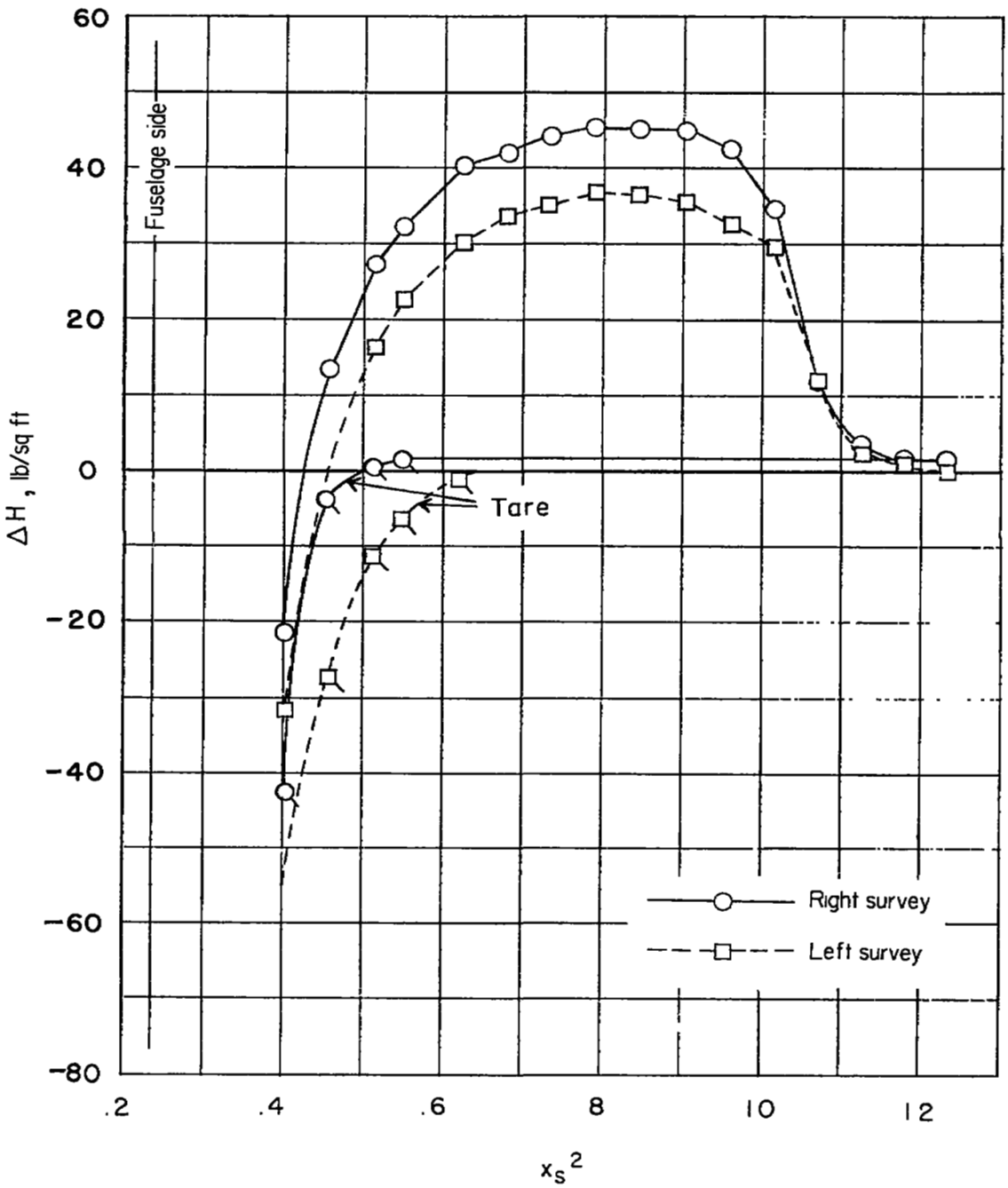

(f) M = 0.85.

Figure 9.- Continued.

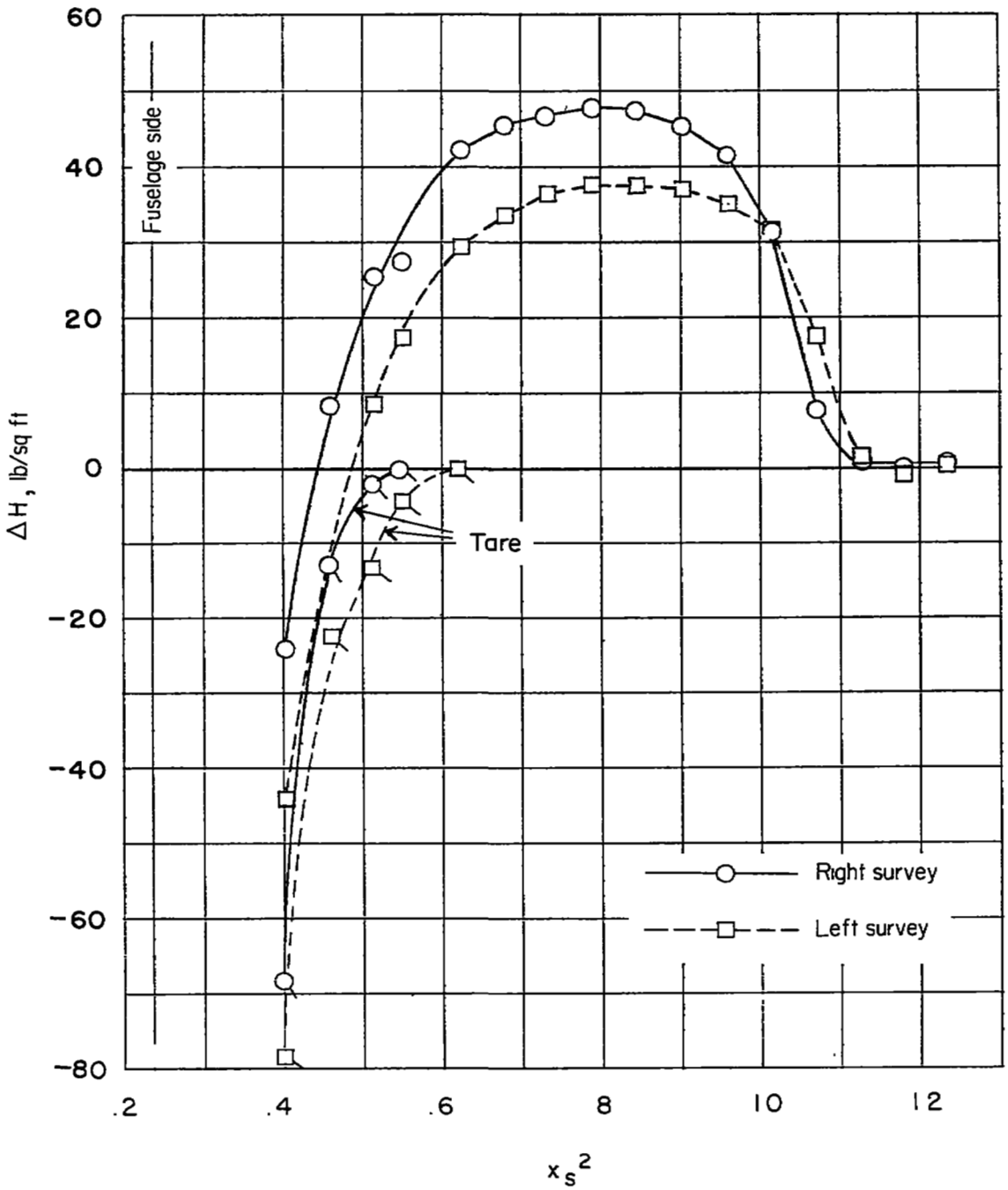

(g) M = 0.90.

Figure 9.- Concluded.

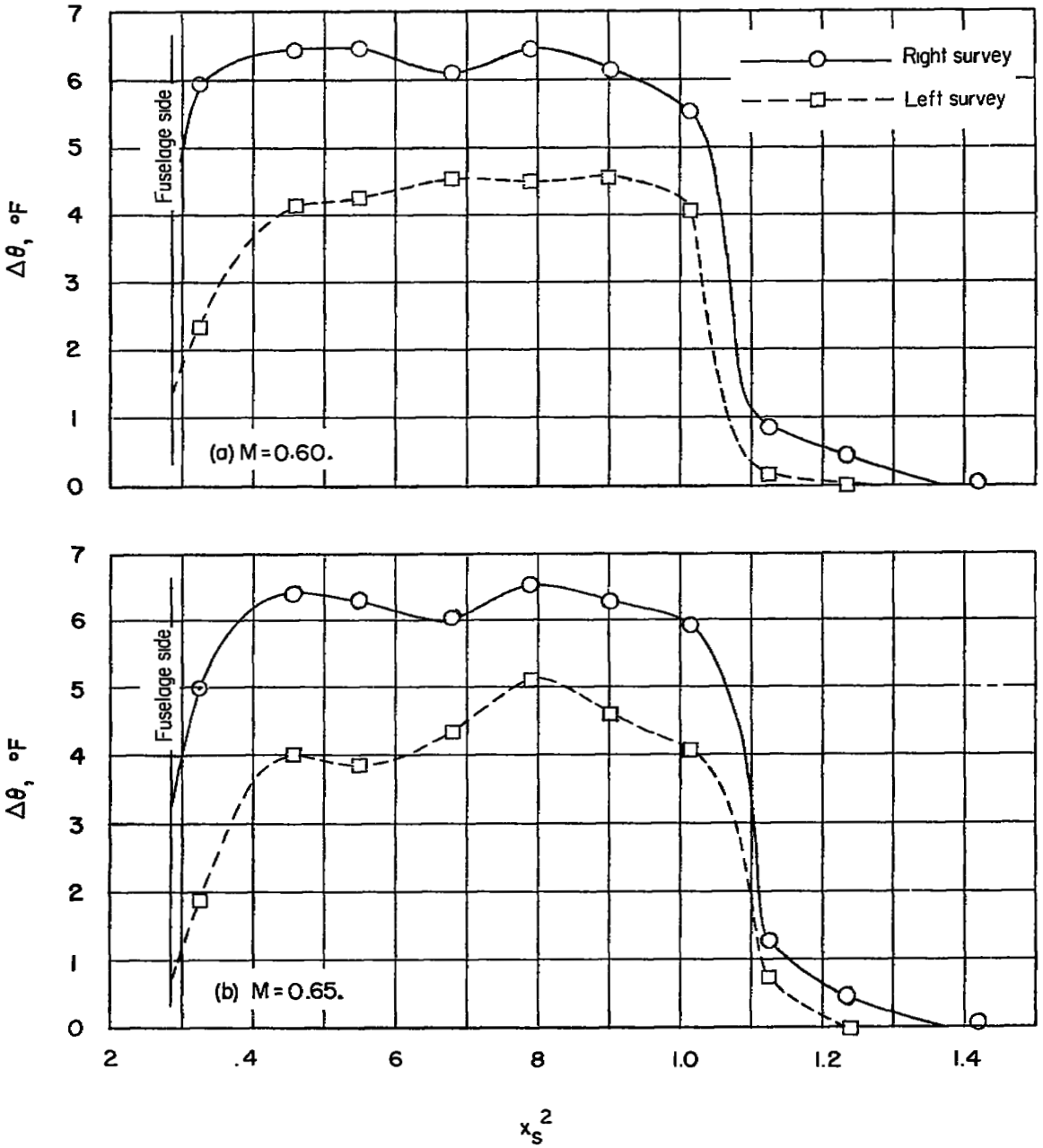

Figure 10.- Distribution of total-temperature rise measured in the propeller slipstream. Propeller and 60° spherical spinner on the propeller research vehicle.

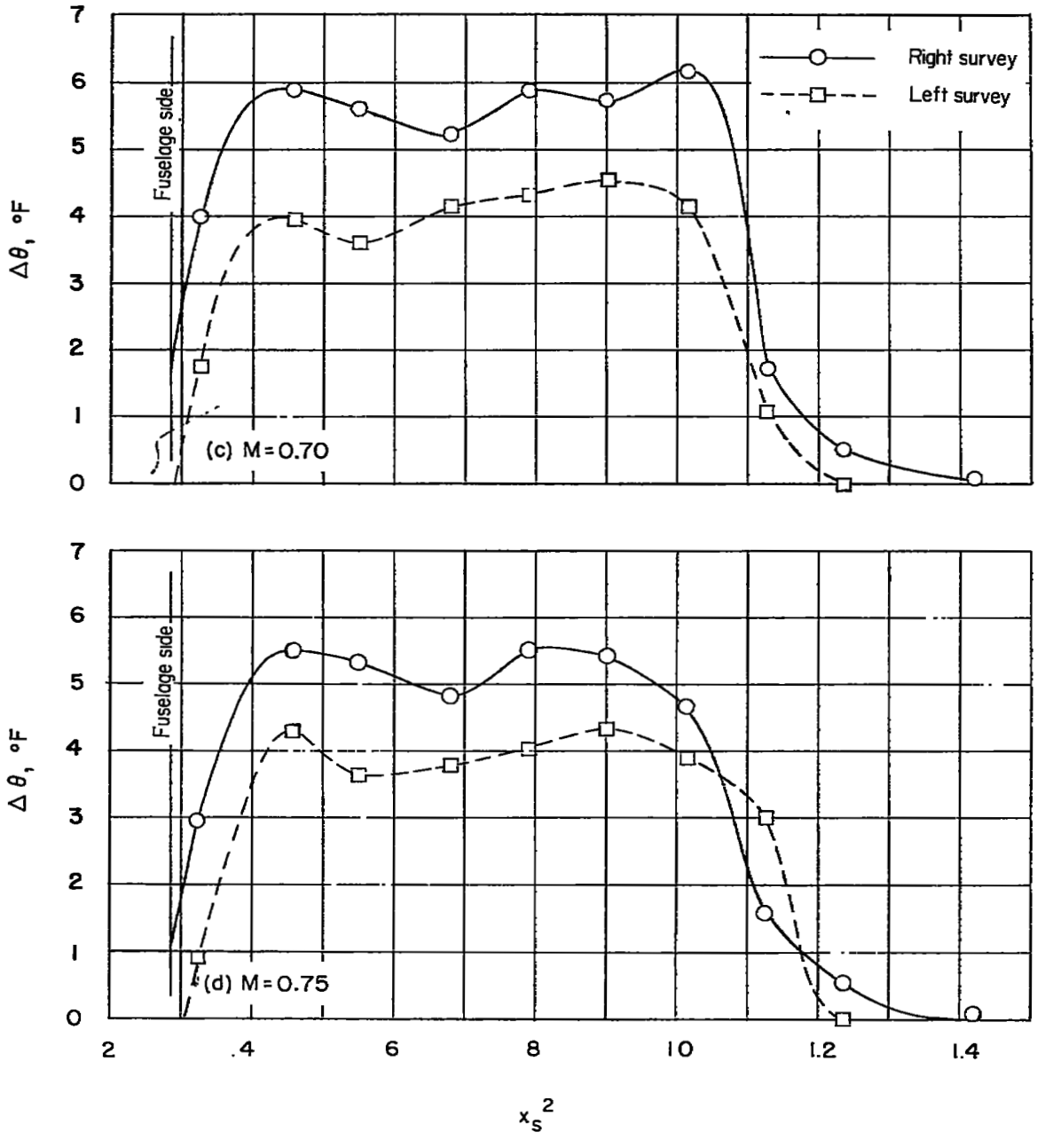

Figure 10.- Continued.

[redacted]

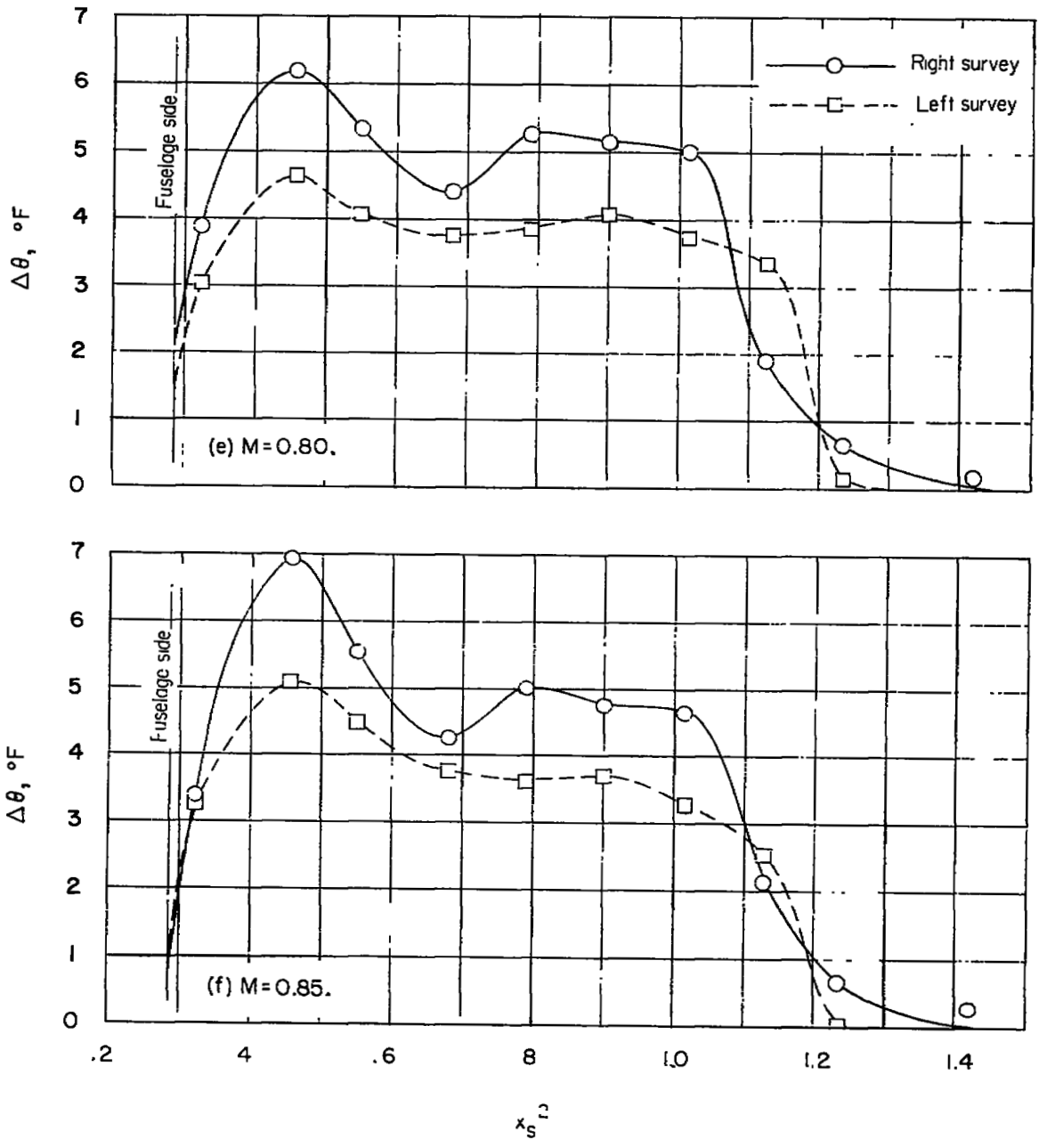

Figure 10.- Continued.

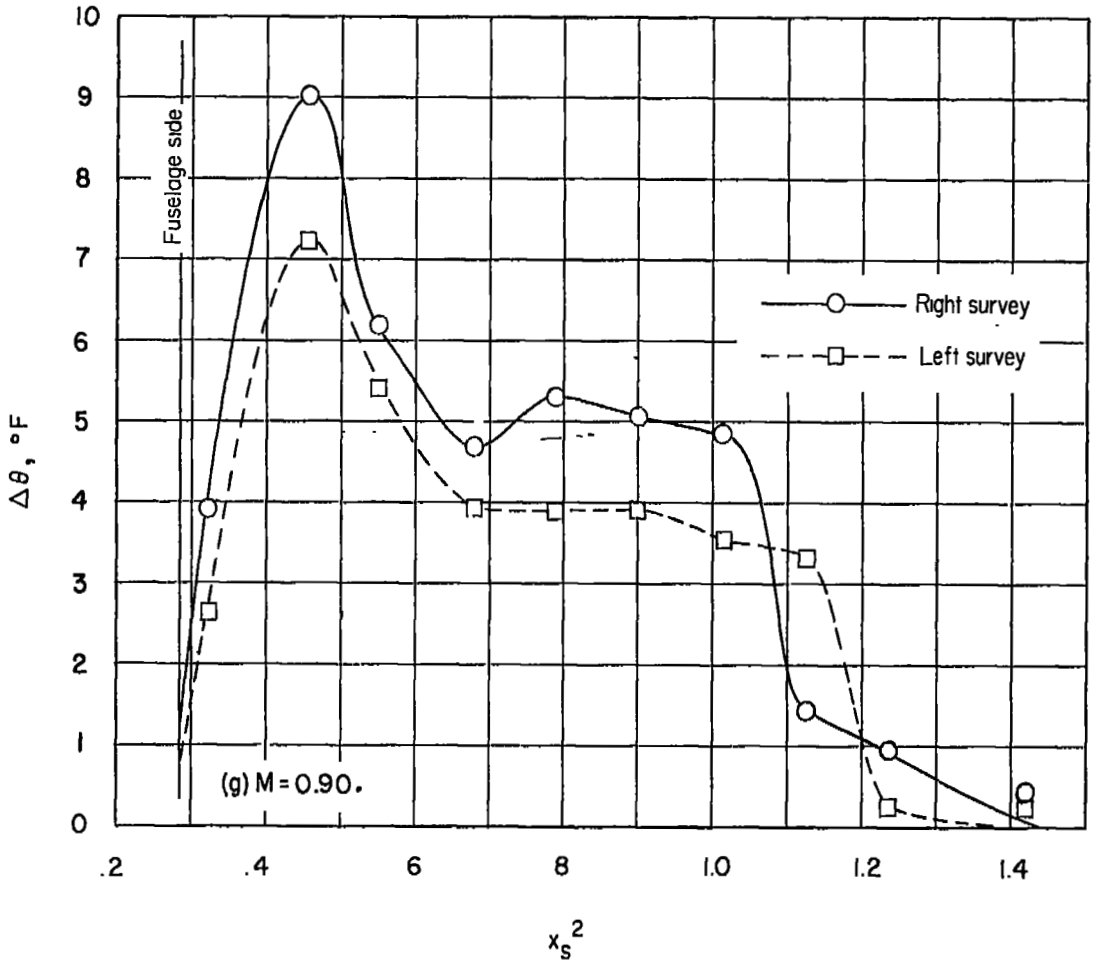

Figure 10.- Concluded.

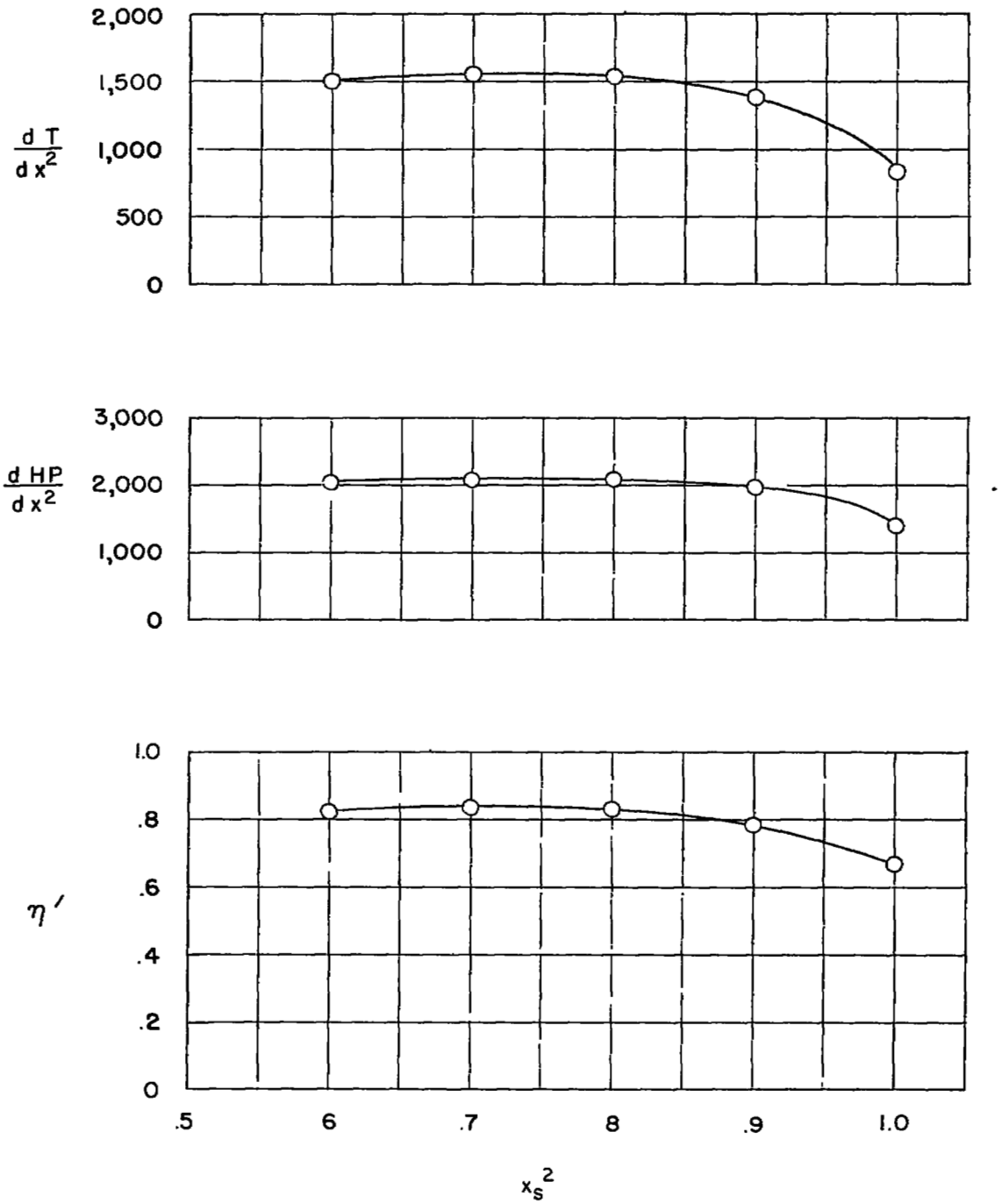

(a) M = 0.60.

Figure 11.- Distribution of section thrust and power, and section efficiency, for the propeller.

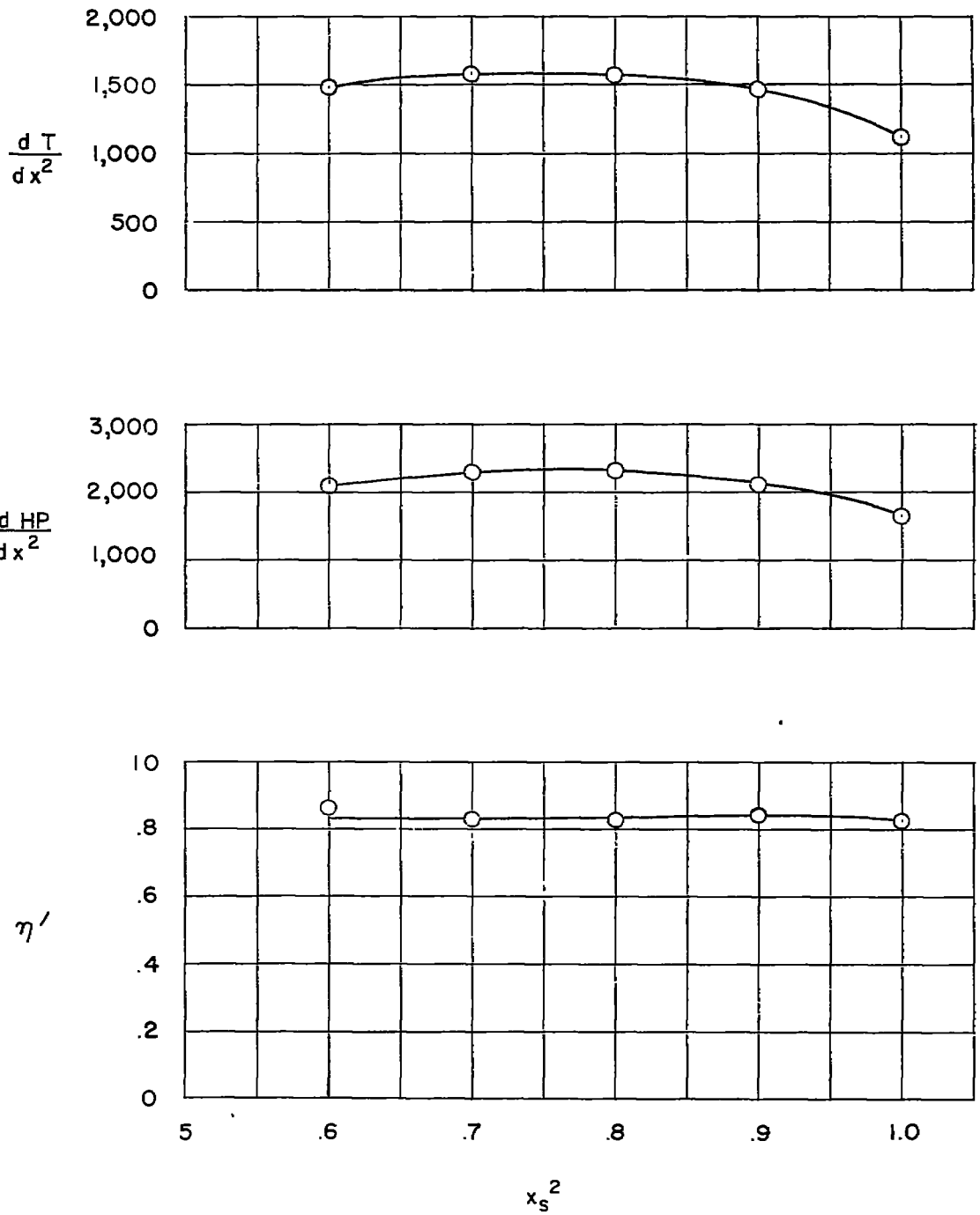

(b) M = 0.65.

Figure 11.- Continued.

[redacted]

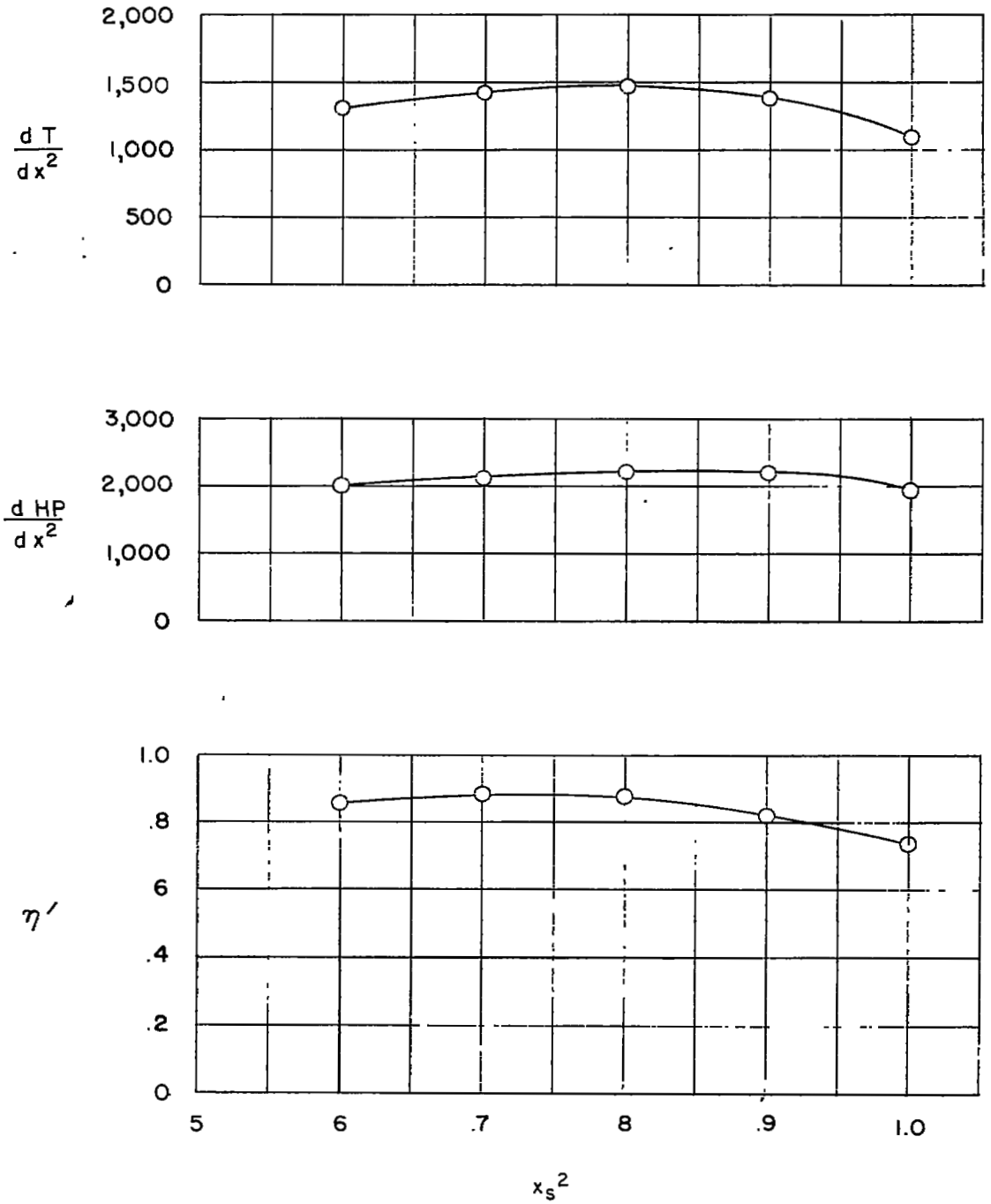

(c) M = 0.70.

Figure 11.- Continued.

[redacted]

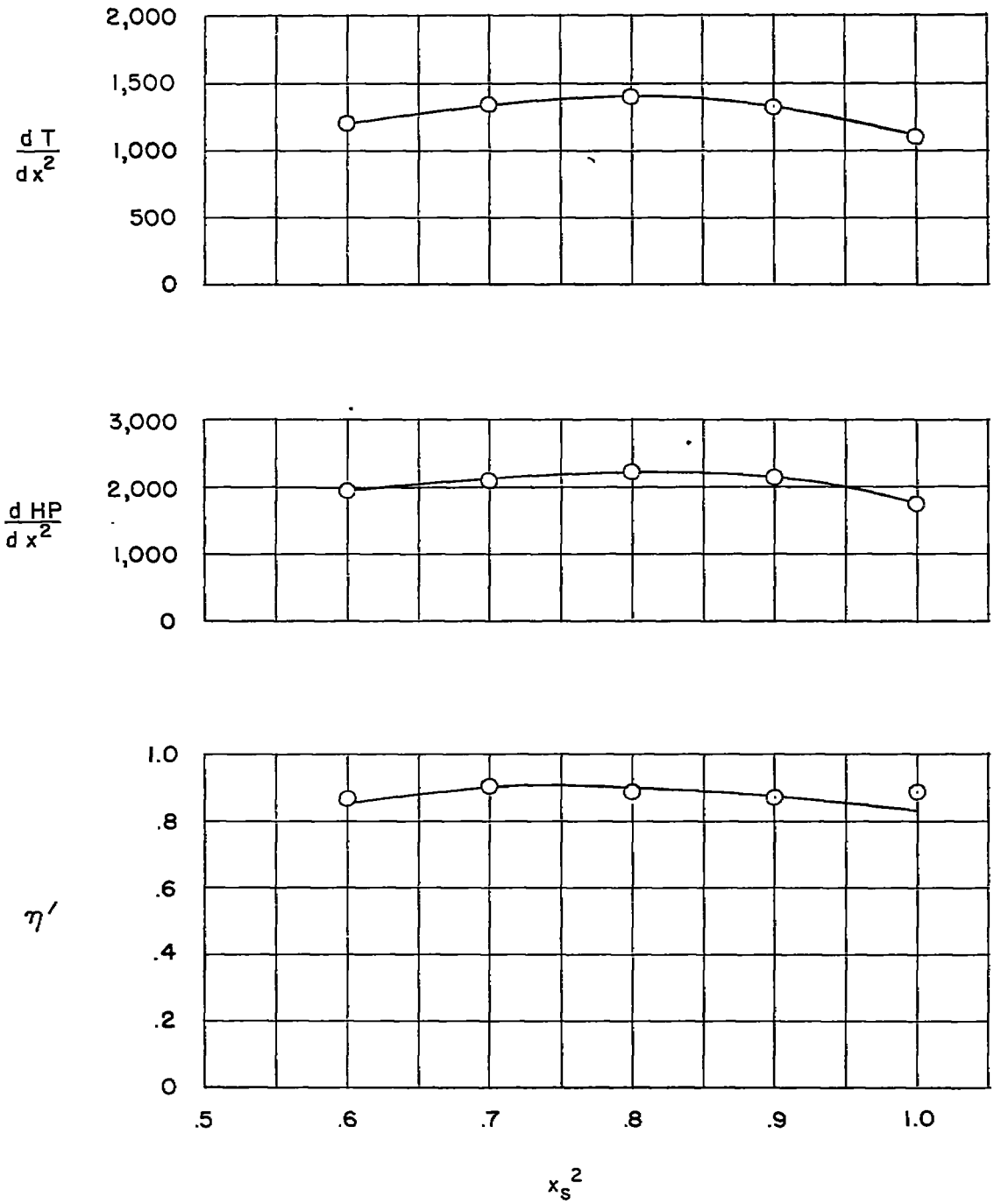

(d) M = 0.75.

Figure 11.- Continued.

[redacted]

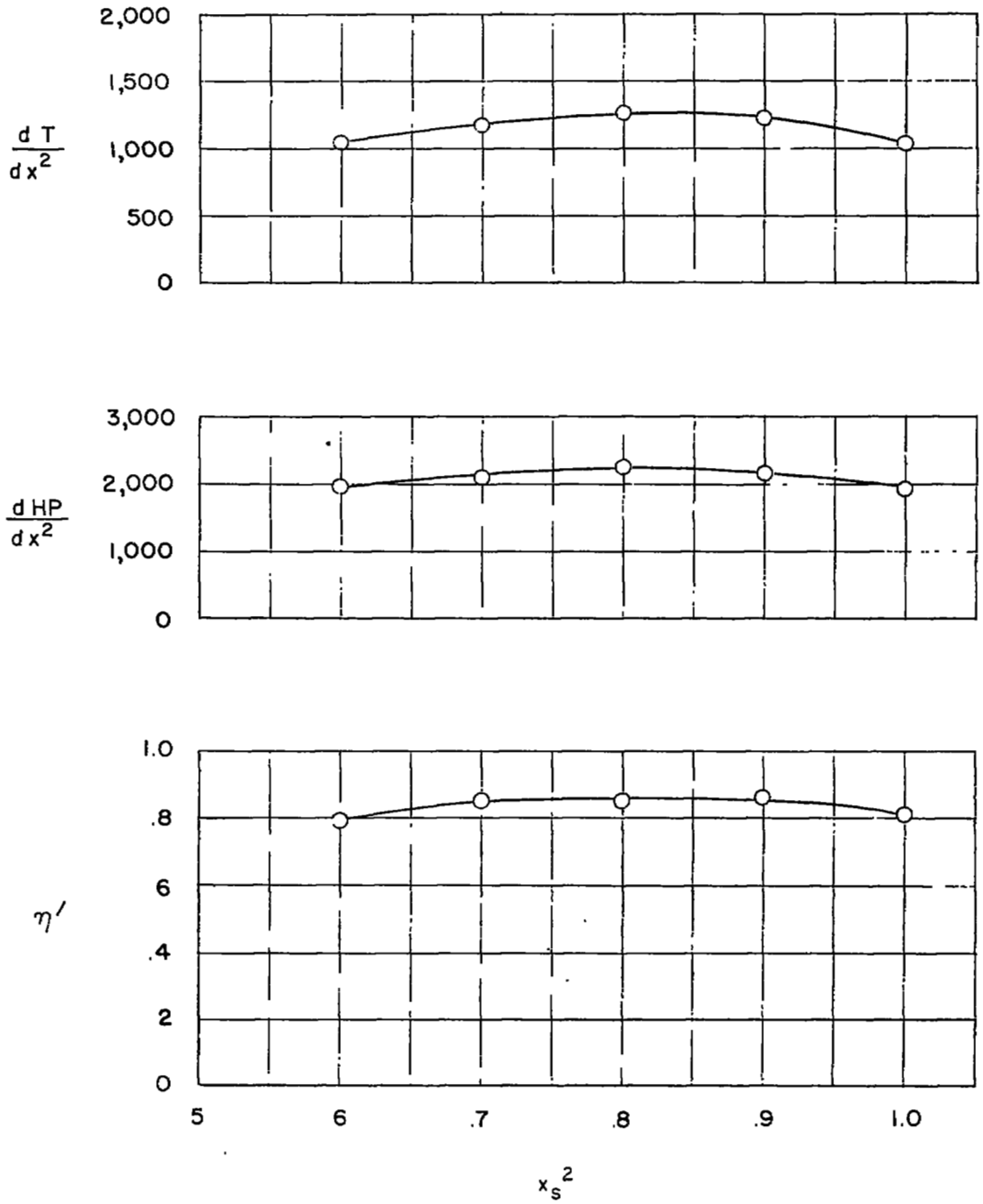

(e) M = 0.80.

Figure 11.- Continued.

[redacted]

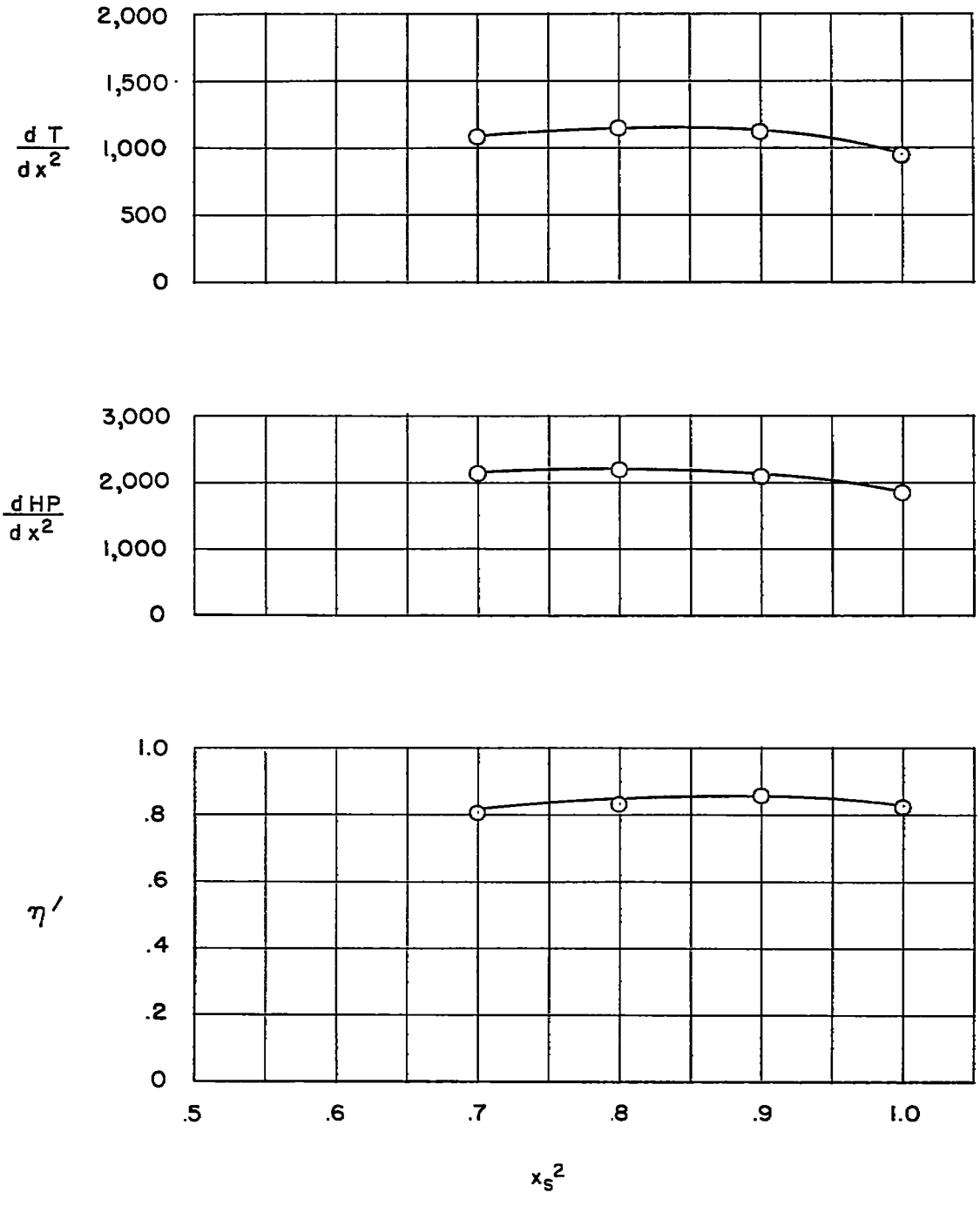

(f) M = 0.85.

Figure 11.- Continued.

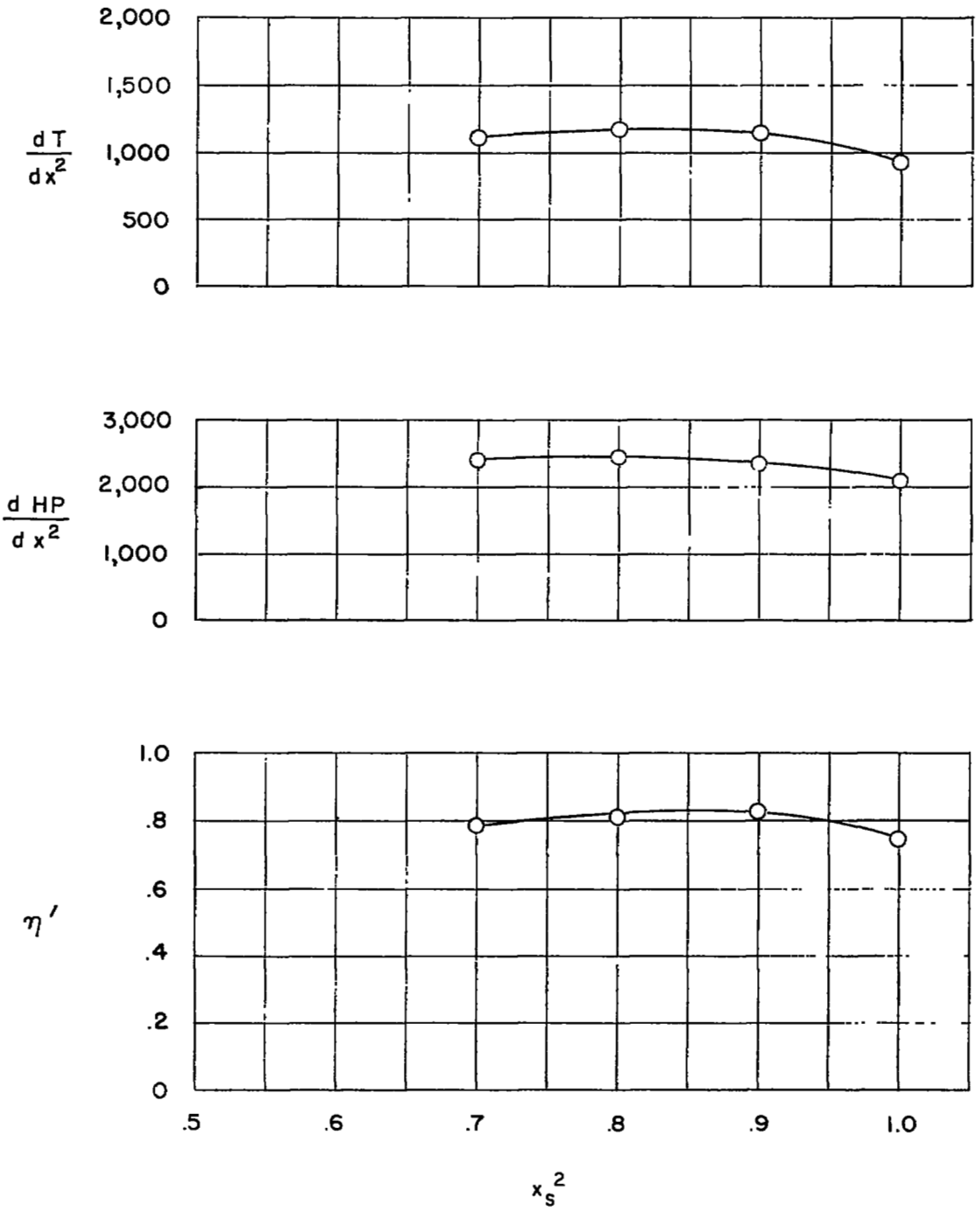

(g) M = 0.90.

Figure 11.- Concluded.

NACA - Langley Field, Va.

[redacted]